



**HAL**  
open science

# Mathematical modelling and assessment of the pH homeostasis mechanisms in while in citric acid producing conditions

Jacqueline García, Néstor Torres

► **To cite this version:**

Jacqueline García, Néstor Torres. Mathematical modelling and assessment of the pH homeostasis mechanisms in while in citric acid producing conditions. *Journal of Theoretical Biology*, 2011, 10.1016/j.jtbi.2011.04.028 . hal-00709547

**HAL Id: hal-00709547**

**<https://hal.science/hal-00709547>**

Submitted on 19 Jun 2012

**HAL** is a multi-disciplinary open access archive for the deposit and dissemination of scientific research documents, whether they are published or not. The documents may come from teaching and research institutions in France or abroad, or from public or private research centers.

L'archive ouverte pluridisciplinaire **HAL**, est destinée au dépôt et à la diffusion de documents scientifiques de niveau recherche, publiés ou non, émanant des établissements d'enseignement et de recherche français ou étrangers, des laboratoires publics ou privés.

## Author's Accepted Manuscript

Mathematical modelling and assessment of the pH homeostasis mechanisms in *Aspergillus niger* while in citric acid producing conditions

Jacqueline García, Néstor Torres

PII: S0022-5193(11)00228-1  
DOI: doi:10.1016/j.jtbi.2011.04.028  
Reference: YJTBI6459



[www.elsevier.com/locate/jtbi](http://www.elsevier.com/locate/jtbi)

To appear in: *Journal of Theoretical Biology*

Received date: 21 July 2010  
Revised date: 16 April 2011  
Accepted date: 23 April 2011

Cite this article as: Jacqueline García and Néstor Torres, Mathematical modelling and assessment of the pH homeostasis mechanisms in *Aspergillus niger* while in citric acid producing conditions, *Journal of Theoretical Biology*, doi:[10.1016/j.jtbi.2011.04.028](https://doi.org/10.1016/j.jtbi.2011.04.028)

This is a PDF file of an unedited manuscript that has been accepted for publication. As a service to our customers we are providing this early version of the manuscript. The manuscript will undergo copyediting, typesetting, and review of the resulting galley proof before it is published in its final citable form. Please note that during the production process errors may be discovered which could affect the content, and all legal disclaimers that apply to the journal pertain.

**Journal of Theoretical Biology**

**Title:** Mathematical modelling and assessment of the pH homeostasis mechanisms in *Aspergillus niger* while in citric acid producing conditions.

**Article type:** regular paper

**Keywords:** pH homeostasis, *Aspergillus niger*, citric acid, mathematical model.

**Corresponding author:** Professor Néstor Torres

**Corresponding author's Institution:** Grupo de Tecnología Bioquímica. Departamento de Bioquímica y Biología Molecular. Facultad de Biología. Universidad de La Laguna. 38206, La Laguna. Tenerife. Islas Canarias. Spain.

**First author:** Jacqueline García

**Abstract**

In this work we introduce an extended model of the *Aspergillus niger* metabolism while in citrate production conditions. The model includes many recent findings related to various transport processes. It now considers new information about the fructose uptake system and the proton and amino acids carriers between cytoplasm and the external medium. It also accounts for recent information about both the malate-citrate antiport between mitochondria and cytoplasm and the dihydrogen citrate ion excretion symport with protons. Finally, the model also accounts for new information about the glycerol-3-phosphate shuttle and pH buffering systems. Provided with this updated representation and after having assessed its quality and dynamic behaviour, we were able to explain the observed pH homeostasis found in *Aspergillus niger* while in citrate producing conditions. The model also serves to enhance our comprehension of the molecular mechanisms operating in order to keep homeostasis of pH in *A. niger* and other fungi, bacteria and yeast of biotechnological relevance.

## Mathematical modelling and assessment of the pH homeostasis mechanisms in *Aspergillus niger* while in citric acid producing conditions

Jacqueline García\* and Néstor Torres\*,<sup>1</sup>

\*Grupo de Tecnología Bioquímica. Departamento de Bioquímica y Biología Molecular. Facultad de Biología. Universidad de La Laguna. 38206, La Laguna. Tenerife. Islas Canarias. Spain.

<sup>1</sup> Corresponding author. Tel: + 34 922 318334. E-mail: [ntorres@ull.es](mailto:ntorres@ull.es).

**Keywords:** pH homeostasis, *Aspergillus niger*, citric acid, mathematical model.

Accepted manuscript

**Abstract**

In this work we introduce an extended model of the *Aspergillus niger* metabolism while in citrate production conditions. The model includes many recent findings related to various transport processes. It now considers new information about the fructose uptake system and the proton and amino acids carriers between cytoplasm and the external medium. It also accounts for recent information about both the malate-citrate antiport between mitochondria and cytoplasm and the dihydrogen citrate ion excretion symport with protons. Finally, the model also accounts for new information about the glycerol-3-phosphate shuttle and pH buffering systems. Provided with this updated representation and after having assessed its quality and dynamic behaviour, we were able to explain the observed pH homeostasis found in *Aspergillus niger* while in citrate producing conditions. The model also serves to enhance our comprehension of the molecular mechanisms operating in order to keep homeostasis of pH in *A. niger* and other fungi, bacteria and yeast of biotechnological relevance.

Accepted manuscript

## 1. Introduction

*Aspergillus niger* fermentation is the world's leading source of commercial citric acid. Citric acid production has been extensively characterized at the molecular level and, consequently, there is readily available information on most of its biochemical, physiological, and genetic aspects [1-7].

The core of this knowledge has been integrated in highly structured dynamical models [8-12]. Since the publication of these models, new data that allow us to improve and extend these models to include other important areas of metabolism have been reported. These data pertain mostly to transport processes [13-15] and metabolic information [6, 7, 16-18]

In this paper, we present an extensive mathematical model of the citric acid metabolism in *A. niger* that, based on previous modeling studies [8, 10], integrates a set of new elements, namely new findings on reactions and processes [3, 19] and homeostasis related contributions [20, 21] with the purpose of analysing the dynamics of pH differences between the environment and the cytoplasmic medium.

Quantification of intracellular pH is a very difficult task and few analyses have been carried out in *A. niger* [52]. However, any process maximization of the citric acid conversion yield at molecular or physiological level should take into account the pH homeostasis mechanisms since many intracellular and protein synthesis processes are susceptible to pH. Thus, given the extraordinary difficulties of the experimental analysis of the pH homeostasis and the importance of the underlying processes for citric acid optimization, we aim to build up a mathematical representation of the pH homeostasis mechanism.

For this purpose we have used the theoretical framework provided by the S-system representation within the power law formalism [8, 9, 22-25]. This representation allows us to study in an intuitive and structured manner how sensitive is the system to changes in independent variables and parameters. These variables and parameters may include the availability of substrates, the strength of the feedback loops, the activities of some enzymes, and the affinity of these enzymes towards their substrates, products or effectors. The model so constructed will provide an integrated vision of the many simultaneous, non linear interactions taking effect. Since it will be submitted to several test quality analysis, including some evaluations of its predictions against experimental evidences, it would become a useful tool in order to support the design of experimental studies and enhance our understanding of the intracellular pH homeostasis.

Our major interest here lies in the role of citrate as an internal molecule overproduced by the fungus as a response to environmental stress conditions [5, 26, 27] and in the role of citrate acting as a buffer contributing to the global homeostasis.

## 2. The model

Figure 1 presents the model, with its reactions and variables. Most of the metabolic processes are described in [10]. It contains thirty one dependent variables as well as several constraint relations assumed as important in the cytoplasmic pH regulation involving citric acid, phosphate and glutamate. On the following pages we will focus on the processes that are new to this version. We introduce the rationale, justification and references that support the choice of the new variables in the following sections.

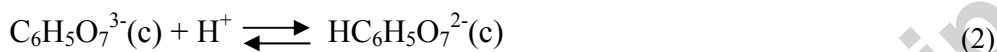
**2.1. Main citrate species.** The three acid groups of citric acid, with *pKa* values of 3.1, 4.7 and 6.4 allow a pH range from acid to almost neutral. According to Burgstaller [21], the following species of citrate can be found in the cytoplasm:  $\text{H}_3\text{C}_6\text{H}_5\text{O}_7$ ,  $\text{H}_2\text{C}_6\text{H}_5\text{O}_7^-$ ,  $\text{HC}_6\text{H}_5\text{O}_7^{2-}$  and  $\text{C}_6\text{H}_5\text{O}_7^{3-}$ . However, given that the *A. niger* internal pH value is 4 units above the first citrate *pKa* [28], the probability of finding significant amounts of fully

protonated citric acid in the cytoplasm is small. Accordingly, only two ionic forms are expected to be found at the cytoplasm: the divalent ion,  $\text{HC}_6\text{H}_5\text{O}_7^{-2}$ , and the trivalent citrate ion,  $\text{C}_6\text{H}_5\text{O}_7^{3-}$ . On the other hand, the amount of the cytoplasmic free protons is small because they are absorbed by the cytoplasmic buffer [29].

**2.2. Citrate transport processes.** The metabolic processes involved in the *A. niger* citric acid synthesis include reactions at the cytoplasm and mitochondrial [5, 19] compartments [6]. The hydrogen citrate ion is excreted from the mitochondria to the cytoplasm in an exchange process that involves cytoplasmic Malate [5]:



This process has been observed both in rat liver mitochondria [30] and in yeast (see review by Karaffa and Kubicek in [5]). In fact, the accumulation of  $\text{MAL}^{2-}(\text{c})$  precedes and collaborates with the citrate production and excretion from mitochondria [30]. The cytoplasmic citrate  $\text{C}_6\text{H}_5\text{O}_7^{3-}(\text{c})$  can then take protons from cytoplasm (2):



The  $\text{H}_2\text{C}_6\text{H}_5\text{O}_7^{-}(\text{c})$  will be excreted out of the cell. We will assume that this citrate excretion occurs via proton symport [21], a mechanism also observed in *E. coli* [31].

In citric acid accumulation conditions the external pH medium value is around 2 [1] and the  $pK_a$  value 3.1, citric acid will mostly appear as an undissociated molecule. However, since the diffusion of undissociated acid from the external medium requires  $\text{Mn}^{2+}$  [14] and this ion is absent in citric acid conditions the diffusion of the undissociated citric acid from the external medium to the cytoplasmic compartment should be considered negligible. This is supported by the observation that in *Candida utilis* citric acid-grown cells, the citric acid diffusion decreases with diminishing external pH [32] and the fact that in *Saccharomyces cerevisiae* and *Hansenula anomala* the cellular permeability by undissociated lactic acid increased along with the pH [33, 34].

**1.3. Metabolite transport processes.** Two glucose transporters have been identified in *A. niger* [13]. Results by Torres et al. [13] and Papagianni and collaborators [35] have shown that these glucose transport processes follow Michaelis-Menten kinetics. However, other authors claim that the process follows passive diffusion [36]. Given the available evidences we have opted for the Michaelis-Menten rate law. On the other hand, we have found in our laboratory (unpublished data) that the fructose-transport system also follows a Michaelis-Menten kinetics, as it has been demonstrated for *Aspergillus nidulans* [37].

Other transport systems like amino acids are also included in the current model, since it has been observed that, in citric acid producing conditions, high amounts of all amino acids are excreted [1]. The current model includes the  $\alpha$ -decarboxylation of L-glutamate to produce 4-aminobutirate (GABA). It has been demonstrated that the GABA synthesis increases with the progress of acidogenic growth [38]. According with this observations, Sander and collaborators suggested that amino acid side chains are an important source of buffering in *Neurospora* and thus could be instrumental in maintaining pH homeostasis [29].

The model considers the glycerol phosphate shuttle as an electron transport mechanism from the cytoplasmic NADH pool to the mitochondrial compartment [39]. It includes the enzyme glycerol-3-phosphate dehydrogenase which has NADH as substrate [40]. Finally, another process considered is the polyol excretion that could contribute to the cytoplasmic pH regulation as a deposit for protons [41].

**2.4. Determination of the cytoplasmic citrate ions concentrations.** Based on the available data and the equilibrium involved, we were able to estimate the different citrate ions species concentrations. Also by using

some of the common procedures in power law formalism (see [24] and [72]), we calculated the kinetic orders and rate constant of the system. Table 1 shows the system parameters and intermediate concentrations used.

**2.5. Intracellular buffering capacity,  $\beta_i$**  A critical feature of the proposed model is the buffer capacity ( $\beta_i$ ) of key intermediates in the control of the pH homeostasis. Buffer capacity is a magnitude that measures the quantity of acid added or subtracted from the cytoplasm [29] by a certain process. In the case of the citrate ions, the cytoplasmic buffer capacity is defined as:

$$\beta_i = 2.303 \cdot K_1 \cdot [X_{29}] \left[ \frac{X_{\text{HC}_6\text{H}_5\text{O}_7^{2-}} + X_{\text{C}_6\text{H}_5\text{O}_7^{3-}}}{(X_{29} + K_1)^2} \right] \quad (3)$$

where  $\beta_i$  is the buffer capacity,  $X_{29}$  is the cytoplasmic proton concentration, and  $X_{\text{HC}_6\text{H}_5\text{O}_7^{2-}}$  the cytoplasmic  $\text{HC}_6\text{H}_5\text{O}_7^{2-}$  concentration.  $K_1$  is the dissociation constant for  $\text{HC}_6\text{H}_5\text{O}_7^{2-}$ .

## 2.6. Model equations

**2.6.1. Mass balance equations.** The dependent variables in this model are characterized by the following equations:

$$dX_1/dt = V_{31,1} - V_{1,2} = V_1^+ - V_1^-$$

$$dX_2/dt = V_{1,2} + V_{3,2} - (V_{2,3} + V_{2,58}) = V_2^+ - V_2^-$$

$$dX_3/dt = (V_{2,3} + V_{4,3} + V_{19,3}) - (V_{3,4} + V_{3,2}) = V_3^+ - V_3^-$$

$$dX_4/dt = (V_{3,4}) - (V_{4,5} + V_{4,3}) = V_4^+ - V_4^-$$

$$dX_5/dt = (V_{4,5} + V_{20,5}) - V_{5,6} = V_5^+ - V_5^-$$

$$dX_6/dt = (V_{5,6} + V_{8,6}) - (V_{6,7} + V_{6,8}) = V_6^+ - V_6^-$$

$$dX_7/dt = V_{6,7} - (V_{7,4} + V_{7,8}) = V_7^+ - V_7^-$$

$$dX_8/dt = (V_{7,8} + V_{6,8} + V_{9,8}) - (V_{8,9} + V_{8,6} + V_{8,44}) = V_8^+ - V_8^-$$

$$dX_9/dt = (V_{8,9}) - (V_{9,8} + V_{9,10}) = V_9^+ - V_9^-$$

$$dX_{10}/dt = (V_{9,10} + V_{11,10}) - V_{10,11} = V_{10}^+ - V_{10}^-$$

$$dX_{11}/dt = V_{10,11} - (V_{11,10} + V_{11,15}) = V_{11}^+ - V_{11}^-$$

$$dX_{12}/dt = V_{14,12} - V_{12,14} = V_{12}^+ - V_{12}^-$$

$$\begin{aligned}
dX_{13}/dt &= (V_{7,13} + V_{17,13}) - (V_{13,14} + V_{13,17}) = V_{13}^+ - V_{13}^- \\
dX_{14}/dt &= (V_{13,14} + V_{12,14}) - (V_{11,15} + V_{14,12}) = V_{14}^+ - V_{14}^- \\
dX_{15}/dt &= (V_{11,15} + V_{14,15} + V_{16,15}) - (V_{15,16} + V_{15,18}) = V_{15}^+ - V_{15}^- \\
dX_{16}/dt &= (V_{15,16} + V_{17,16}) - (V_{16,15} + V_{16,17}) = V_{16}^+ - V_{16}^- \\
dX_{17}/dt &= (V_{16,17}) - (V_{17,16} + V_{17,124}) = V_{17}^+ - V_{17}^- \\
dX_{18}/dt &= \left( V_{15,18} + V_{C_6H_5O_7^{3-}, 18} \right) - \left( V_{18,61} + V_{18, C_6H_5O_7^{3-}} \right) = V_{18}^+ - V_{18}^- \\
dX_{19}/dt &= V_{32,19} - V_{19,3} = V_{19}^+ - V_{19}^- \\
dX_{20}/dt &= (V_{4,5} + V_{21,20}) - (V_{20,21} + V_{20,5}) = V_{20}^+ - V_{20}^- \\
dX_{21}/dt &= (V_{20,21}) - (V_{21,20} + V_{21,23}) = V_{21}^+ - V_{21}^- \\
dX_{22}/dt &= (V_{5,6} + V_{9,8} + V_{21,20} + V_{70,22}) - (V_{8,9} + V_{20,21} + V_{22,70}) = V_{22}^+ - V_{22}^- \\
dX_{23}/dt &= V_{21,23} - V_{23,0} = V_{23}^+ - V_{23}^- \\
dX_{24}/dt &= (V_{26,24} + V_{17,24}) - (V_{24,25} + V_{24,26}) = V_{24}^+ - V_{24}^- \\
dX_{25}/dt &= V_{24,25} - V_{25,GABA} = V_{25}^+ - V_{25}^- \\
dX_{26}/dt &= \left( V_{24,26} - V_{GLU-,26} \right) - V_{26, GLU^-} = V_{26}^+ - V_{26}^- \\
dX_{27}/dt &= V_{HPO_4^{2-},27} - V_{27, HPO_4^{2-}} = V_{27}^+ - V_{27}^- \\
dX_{28}/dt &= (V_{5,6} + V_{6,7} + V_{6,8} + V_{69,28}) - (V_{1,2} + V_{3,4} + V_{7,8} + V_{8,6} + V_{28,63} + V_{19,3}) = V_{28}^+ - V_{28}^- \\
dX_{29}/dt &= \left( V_{18, C_6H_5O_7^{3-}} + V_{27, HPO_4^{2-}} + V_{77,18} + V_{24,25} \right) - \left( V_{1,18} + V_{28,63} + V_{24,26} + V_{25,GABA} + V_{18,61} \right) = V_{29}^+ - V_{29}^- \\
dX_{30}/dt &= (V_{10,11} + V_{13,14} + V_{17,16} + V_{20,21} + V_{22,70}) - (V_{11,10} + V_{16,17} + V_{21,20} + V_{30,51} + V_{70,22}) = V_{30}^+ - V_{30}^- \\
dX_{31}/dt &= V_{23,67} - V_{31,23} = V_{31}^+ - V_{31}^-
\end{aligned}$$

(4)

**2.6.2. S-system equations.** The differential equations in the S-System representation, including the numerical values of the rate constants and kinetic orders with four significant figures, are described in the Supplementary section (Equations S1). The rate constant and kinetic order values were assessed by standard methods [10, 24].

The model dynamic behaviour, steady state and sensitivity analysis were conducted with the software package PLAS<sup>©</sup> [55].

### 3. Results

**3.1. Steady state analysis.** The steady state and stability analysis showed that the basal steady state represented is stable as shown by the negative magnitudes of eigenvalues (Supplementary section; Table S1). The eigenvalues have eight non-zero imaginary parts that should imply potential oscillations of the system [24]. Also, the ranges between the eigenvalues indicate that the dependent variables have different time scales. Thus, after a transient perturbation on some key intermediates (e.g.  $C_6H_5O_7^{3-}$ ;  $X_{15}$ ) the system returns to its original steady state only after a long time, while a perturbation in some other intermediates (e.g.  $H_2PO_4^-$ ;  $X_{27}$ ) takes a shorter time to recover from (see section 3.4.1; Figure 2).

### 3.2. Sensitivity analysis

There are two types of sensitivities, rate constant and kinetics order sensitivities. A rate constant sensitivity is defined as the ratio of a relative change in a dependent concentration,  $X_i$  or flux,  $v_i$ , to a relative change in a rate constant ( $\alpha$  or  $\beta$ ;  $r_j$ ). The corresponding expression is:

$$S(X_i(v_i), r_j) = \left( \frac{\partial X_i(v_i)}{\partial r_j} \frac{r_j}{X_i(v_i)} \right)_0 = \frac{\partial(\log X_i(v_i))}{\partial(\log r_j(v_i))} \quad (5a)$$

where, the subscript 0 refers to the steady state. It can be determined by differentiation of the explicit steady state solution, with respect to the parameter in question. Similarly, the kinetic order sensitivity coefficients are defined as the ratio of a relative change in a dependent concentration,  $X_i$  or flux,  $v_i$ , to a relative change in a kinetic order parameter, ( $g_{jk}$  or  $h_{jk}$ ;  $r_{jk}$ ). The corresponding expression is:

$$S(X_i(v_i), r_{jk}) = \left( \frac{\partial X_i(v_i)}{\partial r_{jk}} \frac{r_{jk}}{X_i(v_i)} \right)_0 = \frac{\partial(\log X_i(v_i))}{\partial(\log r_{jk}(v_i))} \quad (5b)$$

Logarithmic gains are a type of sensitivity coefficients representing the percentage change in a dependent metabolite concentration,  $X_i$ , (or flux,  $v_i$ ) caused by a change in an independent variable,  $X_j$ . They are represented by the following equation:

$$L(X_i(v_i), X_j) = \left( \frac{\partial X_i(v_i)}{\partial X_j} \frac{X_j}{X_i(v_i)} \right)_0 = \frac{\partial(\log X_i(v_i))}{\partial(\log X_j)} \quad (6)$$

Sensitivity analysis offers a characterization of the quality of a model, since it indicates whether the model is able to endure structural changes.

A systematic sensitivity analysis of the model performance in terms of both the sensitivities and logarithmic gains was carried out. There are 961 metabolite rate constant sensitivities and 10757 metabolite kinetic order sensitivities and the same number in its flux counterparts. Regarding the logarithmic gains, the corresponding figures are 1457, respectively. An evaluation of its absolute magnitudes is shown in Table 2. In this Table it can be seen that 63% of the sensitivities are below 1 in both cases; this percentage rises to 95% if we consider values below 10. The examination of the absolute values of logarithmic gains shows a similar pattern, but even more pronounced: 76% are below 1 and 99% below 10. All together, these results indicate that, in spite of some uncertainties, the model can be considered robust enough and well defined.

Because we are primarily interested in the logarithmic gains of metabolites and fluxes directly related to citrate with respect to citrate accumulation and excretion, the influence of the cytoplasmic citrate  $\text{HC}_6\text{H}_5\text{O}_7^{2-}$  transport system ( $X_{61}$ ) and the mitochondrial  $\text{MAL}^{2-}\text{-CIT}^{3-}$  transport system ( $X_{64}$ ) on the metabolites and fluxes involved in citrate synthesis was analyzed in detail.

**3.2.1. Citrate metabolite logarithmic gains.** The most relevant results of this analysis are shown in Table 3. First, it is observed that an increase in  $X_{61}$ , the cytoplasmic citrate transport system causes a general decrease on the glycolytic metabolite concentrations having the largest influence on the mitochondrial pyruvate (-59.55). This very high sensitivity value, as in the event of any other similar situation, suggests that the process is probably not well modelled enough. But if this value is of any significance, it would indicate a significant coupling of the cytoplasmic citrate transport system activity with both the glycolysis and the mitochondrial pyruvate metabolism.

### Referencia al requerimiento de análisis sistemático de las sensibilidades

In this vein, it should be noted that that this perturbation causes a significant change in the same direction (3.367) in the cytoplasmic citrate concentration ( $X_{18}$ ); the same case being observed with the mitochondrial citrate ( $X_{15}$ ) perturbation (0.709). Finally, it is noted that the same profile, but of opposite sign is observed when the perturbation is in the  $X_{64}$  thus indicating opposite influences.

**3.2.2. Flux logarithmic gains.** Table 4 shows the most significant results obtained. Changes in both carriers showed an effect on the glycolytic fluxes. Thus, an increase in  $X_{61}$  causes a general decrease on the glycolytic fluxes, which has the largest influence, again, on the flux through mitochondrial pyruvate ( $X_{13}$ , -11.99). As stated before, this high sensitivity value suggests that the process is probably not well modelled enough. Similarly to the instances observed for the logarithmic gains of metabolite concentrations, the logarithmic gains of the fluxes most affected (negatively) by a perturbation in  $X_{61}$  are those involved in the citrate mitochondrial synthesis together with the flux through malate,  $X_{10}$  and mitochondrial oxaloacetate,  $X_{11}$ . Again, the same profile, but of opposite sign is observed when the perturbation occurs in the  $X_{64}$ , thus indicating opposite influences. Finally, it should be noted that the high logarithmic gains observed could be an indication of some ill-defined model features or parameter values, thus suggesting the necessity of further modifications and assessment.

### 3.4. Dynamic characterization of the system

In this series of explorations two types of experiments were carried out. In some instances (Sections 3.4.1, 3.4.2 and 3.4.3) some intermediate concentrations (Figures 2 and 4) were changed, in independent pulse experiments in which at time 50 minutes the dependent variable was changed from its initial steady state value to a reduced value and the system evolution subsequently monitored. In another series of perturbation experiments, starting from the citric acid producing steady state, the basal value of a parameter was kept constant from minute 50 until minute 100 at a decreased value from its original one and the system time evolution monitored (Figures 3, 5 to 8).

**3.4.1. Change in cytoplasmic metabolite concentrations.** In Figure 2A it can be seen that when the mitochondrial citrate,  $\text{C}_6\text{H}_5\text{O}_7^{3-}\text{m}$  ( $X_{15}$ ) concentration was temporarily decreased,  $\text{PYRc}$  ( $X_7$ ) and  $\text{H}^+$  ( $X_{29}$ ) increased while  $X_{15}$  and  $X_{18}$  reacted decreasing their concentration. Later, it was observed that the glycolytic intermediates  $X_7$  decreased while  $X_{18}$  increased considerably. In the same Figure (2B) it is shown the evolution of intracellular pH. As it can be noticed, after a sudden decrease the steady state value then recovers at the same pace as  $X_{18}$ . However, after some pulse experiments with  $\text{HC}_6\text{H}_5\text{O}_7^{2-}$  ( $X_{18}$ ; Figure 2C), it was observed that after decreasing  $X_{18}$  concentration by a 95%, the glycolytic metabolites  $X_7$  increased their values from one to three-fold and the cytoplasmic concentration of  $\text{H}^+$  ( $X_{29}$ ) increased about seven-fold. At the end of

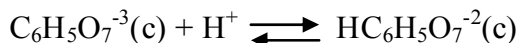
the perturbation the glycolytic metabolite  $X_7$  returned to the original values while  $X_{18}$  increased and  $X_{29}$  decreased. On the other hand,  $H_2PO_4^-$  ( $X_{27}$ ) showed some fluctuations before returning to its initial values.

In another pulse experiment, after decreasing by 70% the concentration of the reduced cytoplasmic phosphate  $H_2PO_4^-$ , ( $X_{27}$ , see Figure 2D), a rapid transient decrease in  $X_{18}$  and  $X_{29}$  is observed, together with an increase in  $X_7$ . Once the perturbation ended, the cytoplasmic metabolites  $X_7$  and  $X_{29}$  decreased while the mitochondrial metabolite  $X_{18}$  increased. Kubicek [1] showed a similar regulatory effect of phosphate, but this effect was found when phosphate was decreased in the citrate production medium.

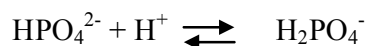
**3.4.2. Dynamics of the cytoplasmic pH.** In a previous section we showed that both the cytoplasmic citrate transporter ( $X_{61}$ ) and the mitochondrial  $MAL^{2-}$ - $CIT^{3-}$  transporter ( $X_{64}$ ) are important parameters in the control of key metabolites. In this section we will present the observed influence on the intracellular pH of changes in these two parameters as well as of the changes in the alternative respiratory system ( $X_{51}$ ) and the  $H^+$ -ATPase ( $X_{63}$ ).

Figure 3A shows the results when the cytoplasmic citrate transport,  $X_{61}$  was changed. We observe a significant initial increase of 0.4 pH units. The reduction of the  $X_{61}$  activity causes the citric acid accumulation within the mitochondria citric which, by taking protons, increases the cytoplasmic pH. In Figure 3B, after inhibition in the mitochondrial  $MAL^{2-}$ - $CIT^{3-}$  transport system,  $X_{64}$ , the pH drops 0.6 pH units, but after this perturbation the pH recovers its initial value after reaching a maximum pH value of 7.9. All the above together indicates that in all cases, but to a somewhat lesser extension in the cases of the cytoplasmic citrate transport ( $X_{61}$ ) and the mitochondrial  $MAL^{2-}$ - $CIT^{3-}$  transports system, ( $X_{64}$ ) the system is able to keep the cytoplasmic pH well within physiological ranges against any significant variation in key parameter values. Figure 3C shows the pH dynamics after a perturbation of the alternative respiratory system,  $X_{51}$ . It is observed that the intracellular pH shows a small decrease, returning to the previous steady state value after a minimum oscillation. In practical terms it can be said that the system is almost insensitive to this perturbation. In the case of the  $H^+$ -ATPase,  $X_{63}$ , pH initially drops, but then increases 0.1 units, slowly returning then to its previous value (Figure 3D).

**3.4.3. Dynamics of the citric acid and phosphate buffer capacity.** Here, starting from the citric acid-producing steady state, the variables citrate,  $HC_6H_5O_7^{2-}$  ( $X_{18}$ ), and phosphate,  $H_2PO_4^-$  ( $X_{27}$ ), concentrations were decreased, in an independent pulse experiment, at time: 5 min., from its initial value to 5% of their original value (Figure 4). It should be taken into account that given that the sum of  $HC_6H_5O_7^{2-}$  and  $C_6H_5O_7^{3-}$  is a system parameter ( $X_{73}$ ) the perturbation in  $X_{18}$  is simultaneous with a change in  $C_6H_5O_7^{3-}$  so that  $X_{73}$  would remain constant. The same applies to the changes in  $X_{27}$  and  $HPO_4^{2-}$  concerning  $X_{75}$ . Then, the evolution of the buffer capacity ( $\beta_i$ ) of each buffer component, the intracellular pH and the buffer components were monitored (Figure 4). The buffer capacity of each case is given by the following equilibrium:



for the citrate buffer, and by the equilibrium



for the phosphate buffer.

In Figure 4A it can be seen that the citrate  $\beta_i$  showed a sharp decrease of almost 15 units after a perturbation in  $HC_6H_5O_7^{2-}$ , but quickly returned to its original value. The phosphate buffer capacity (Figure 4B) also shows a decrease after the perturbation in the  $H_2PO_4^-$  concentration. All together, these observations indicate that the dynamics of the cytoplasmic pH is influenced by both, the citrate and phosphate concentrations but at the same time displays a strong recovery capacity.

#### 3.4.4. Effects of changes in the alternative respiratory system.

When in stress conditions for citric acid production, an alternative respiratory system is also active in *A. niger*, in addition to that sensitive to cyanide: the salicylhydroxamic acid-sensitive system [60, 74]. In Figure 5 it is represented the evolution of some representative system variables after a 60% inhibition of the alternative respiratory system ( $X_{51}$ ). A decrease in CoA ( $X_{12}$ ) and acetyl-CoA ( $X_{14}$ ) was observed while mitochondrial pyruvate ( $X_{13}$ ) and mitochondrial  $\text{NAD}^+$  ( $X_{30}$ ) increased their values. The latter ones exhibited more than a four- and seven-fold increase, respectively, before reaching their initial value.  $X_{13}$  accumulation suggests that the alternative respiratory inhibition is affecting the mitochondrial pyruvate kinase since a decrease in its products, CoA and acetyl-CoA, is observed. On the other hand, the increase in mitochondrial  $\text{NAD}^+$  could indicate an excess of mitochondrial NADH that was also not oxidized by the respiratory chain. Some experimental evidences [59] show that the interruption in aeration negatively affects the citric production in *A. niger*. In the same vein, Rohr and collaborators observed a lesser oxygen uptake at an early phase when compared with the late stage of fermentation, when the citric acid production starts [58]. There are changes on the cytoplasmic pH as well as in several dependent variables, but in all cases they return to their original steady state.

**3.4.6. Effects of down-regulation in the cytoplasmic citrate carrier and mitochondrial malate-citrate transport system.** Figure 6A shows the system dynamics after a 60% decrease in the cytoplasmic citrate transport  $X_{61}$ . It can be seen that it causes a twofold accumulation of  $X_{18}$  and a decrease of  $X_7$  and  $X_{13}$ . The protons,  $X_{29}$ , showed a fluctuation pattern. The excretion from the cytoplasmic compartment to the external medium of  $\text{HC}_6\text{H}_5\text{O}_7^{2-}$ ,  $X_{18}$ , could be a process without energy consumption [12]. In the current model the citrate excretion occurs via the  $\text{HC}_6\text{H}_5\text{O}_7^{2-}/\text{H}^+$  symport, which allows the citrate translocation out of the cell with an additional efflux of protons. This perturbation stimulated metabolic fluctuations. Mitochondrial and citric acid pyruvate did also accumulate.

Figure 6B shows the systems dynamics after a similar perturbation, but in the mitochondrial malate-citrate transport ( $X_{64}$ ). It is observed an initial increase decrease in  $X_{18}$ , but there is a decrease of some glycolytic metabolites ( $X_7$ ) as well as other cytoplasmic intermediates such as  $X_{13}$  and  $X_{29}$ . It has been showed that the  $\text{C}_6\text{H}_5\text{O}_7^{3-}$  could be excreted across the mitochondrial membrane through a specific transport [61]. This transport is related with the oxaloacetate produced in the cytoplasmic compartment when it is reduced to malate by cytoplasmic malate dehydrogenase and goes to the mitochondrial space by an antiporter malate-citrate transport [5].  $\text{C}_6\text{H}_5\text{O}_7^{3-}$  and  $\text{MAL}^{2-}$  are substrates of the mitochondrial transporter [62]. As it has been mentioned above, this model considers that the mitochondrial citrate transport only takes the form of  $\text{C}_6\text{H}_5\text{O}_7^{3-}$  and malate  $\text{MAL}^{2-}$ . It was reported a new but similar dicarboxylate-tricarboxylate transport that accepts both anions,  $\text{C}_6\text{H}_5\text{O}_7^{3-}$  and  $\text{MAL}^{2-}$ , that also catalyzes the exchanges between the cytoplasmic and mitochondrial compartments [63].

**3.4.7. Effects of the changes in the  $\text{H}^+$ ATPase.** Figure 7 shows the system dynamics after a 60% decrease in the  $\text{H}^+$ ATPase,  $X_{63}$ . It can be seen that  $\text{HC}_6\text{H}_5\text{O}_7^{2-}$ ,  $X_{18}$  and the  $\text{H}^+$  concentration,  $X_{29}$ , increase before returning to their original values where a decrease of  $X_{17}$  was also observed. It has been reported [6] that at the late growth phase, in some *A. niger* strains, the  $\text{H}^+$ ATPase could be not responsible for all the proton extrusion to cytoplasm. The small increase in the proton concentration observed here could indicate that other pH regulatory mechanisms are operating.

An experimental verification of the model prediction was provided by the results obtained by Jernejc and Legisa [27]. These authors showed that changes in the  $\text{H}^+$ -ATPase were followed by a spontaneous drop of intracellular pH in a high citric acid-producing *A. niger* strain. In particular, these authors showed that addition of vanadium ions, potent inhibitors of  $\text{H}^+$ -ATPases, to the culture medium, not only induces an enhanced citric acid accumulation but also a reduced intracellular pH, thus suggesting that one of the mechanisms stimulating

citric acid accumulation by *A. niger* could be a slight cytoplasmic acidification. An equivalent perturbation experiment carried out with our model (see Figure 7) shows that any inhibition of the  $H^+$ -ATPases is followed by a cytoplasmic acidification, thus in agreement with the experimental observations.

#### 4. Discussion

In this work we have built up a mathematical model with the aim of relating the citrate excretion in *A. niger* with the cytoplasmic pH regulation. That model suggests that *A. niger* requires the citric acid intracellular accumulation and its excretion to regulate the cytoplasmic pH against external acidic conditions. The results also serve to illustrate how excretion to the medium could be a general mechanism for internal pH regulation.

There is a mechanism that arises as critical in the pH homeostasis in *A. niger*. Citrate and phosphate buffer capacity decreases when citrate anion  $C_6H_5O_7^{3-}$  concentration decreases. Thus, any such perturbation alters the cytoplasmic pH, but the buffer capacity soon recovers as the citrate  $HC_6H_5O_7^{2-}$  concentration increases. Other key elements are the transport systems. The model predicts the behaviour of the system after changes in both the cytoplasmic and mitochondrial citrate transport systems. Significantly, when the cytoplasmic citrate transport is increased, it causes the accumulation of the cytoplasmic citrate but without affecting the internal pH and while also having a small effect on the mitochondrial citrate. On the other hand activation of the mitochondrial citrate transport enhances the mitochondrial  $\alpha$ -keto-glutarate export to the cytoplasm.

The sensitivity analysis carried out for the citrate transport systems involved are another important source of information provided by the model. The cytoplasmic citrate concentration increases its concentration and its flux if the citrate cytoplasmic transport increases, while an increase in the mitochondrial transport produces an opposite effect in the cytoplasmic citrate flux. Overall, these findings support the idea of the important role that mitochondrial and cytoplasmic citrate transports play in the citrate accumulation process.

Another aspect that our model allows to explore is the effect on the pH and citrate accumulation of changes in the glucose uptake and in some enzymes. Accordingly, it has been shown that a 10% activation in the external glucose transport causes a general enhancement of the glycolytic intermediates as showed by our model. However, our model does not show any increase in mitochondrial and cytoplasmic citrate. We have also concluded that the cellular glycolytic requirements can be modulated by the citrate excretion either from the mitochondrial or cytoplasm. This fact has been experimentally observed in *A. niger* transformants [64].

The present model shows that citrate accumulates when the  $H^+$ -ATPase activity is reduced (Figure 7). In this vein, experimental results indicate that a fourfold increase in the  $H^+$ -ATPase activity by in an A158 *A. niger* strain correlates with a low citric acid production [27]. It has been observed that  $H^+$ -ATPase inhibition raises the medium pH. However, our model assumes a constant, acidic pH. As result of the  $H^+$ -ATPase perturbation, the cytoplasmic pH slightly decreases but the ATP concentration remains unaffected. It is thus proposed, in agreement with some observations, [7] that since during citric acid synthesis the ATP requirements are met by the glycolytic pathway, a higher ATP concentration can have a negative effect on glycolytic flux. This model contemplates that an increase of the cytoplasmic proton concentration by a decrease in the  $H^+$ -ATPase causes an increase of the citrate intracellular accumulation as observed in root cells [65]. However, we cannot discard this as not being the effect of a passive citric acid efflux parallel to the  $H^+$  efflux driven by the plasma membrane  $H^+$ -ATPase.

The trivalent anion  $C_6H_5O_7^{3-}$  efflux from the mitochondrial compartment through a transport system was demonstrated in yeast [66]. Later, the acid is excreted outside of the cell through a transport system [14]. The stoichiometry of this process could vary with the dissociation state of the transport system, as was found in membrane vesicles in *E. coli* [67]. We can speculate if in *A. niger* the dissociation state of the citric acid transport is linked to the external pH. The divalent citrate excretion/proton symport,  $HC_6H_5O_7^{2-}/H^+$  could be possible if we are to assume that the citrate divalent anion is excreted down its potential gradient and the

protons are moving against it. In the external medium the pH is around 2. At this value the membrane permeability is small for the undissociated acid [32]. This low pH does not permit the diffusion of the undissociated citric acid to enter the cells. Furthermore, the *A. niger* cytoplasmic pH has a small probability of releasing undissociated organic acids. Although it was not considered here, it is possible to find the citrate under physiological conditions in two dissociated  $Mg^{2+}$  complexes such as:  $MgH_2C_6H_5O_7^-$  and  $MgHC_6H_5O_7^{2-}$  [68].

Additionally, the model included the process of excretion and re-consumption of other organic metabolites like glutamate. Glutamate is transformed into 4-aminobutyrate by a decarboxylation reaction and then excreted to the medium. Our model showed no significant changes in the level of these metabolites. However, the associated logarithmic gains reflect an influence of the external proton concentration on the glutamate, 4-aminobutyrate and the external glutamate.

As indicated above, the experimental assessment of the great amount of variables involved in the study of pH homeostasis is a very difficult and time-consuming task. In situations like these, the previous analysis of the system under consideration becomes indispensable if we want to save efforts and resources. It is at this point that the modelling approach becomes instrumental in dealing with complex problems like the present one. In fact we have obtained a pragmatic, *a posteriori* verification of the model predictions (see section 3.4.7) which supports the proposed approach.

One of the main tenets of the Systems Biology approach is the integration of the system information previously gathered in a mathematical model susceptible to be analysed. From the system insights so obtained it is thus possible to decide what variables are relevant to consider and which parameters are worthwhile to measure and modulate.

In spite of the model limitations, we believe that the new inclusions make a more realistic model for the description of the pH homeostasis mechanism. The current model is the result of a process of making simplifying assumptions where many simultaneously variables interact in a non-linear form. We are confident that it could be instrumental in getting insights on the critical factors involved in this mechanism and greatly facilitate its optimization by using readily available optimization methods ([69-71], work in progress). Finally we think that this model could serve as the basis of an evolving testing bench where other analysis can be carried out in addition to those here presented.

## Acknowledgements

The authors want to acknowledge the excellent work done by the two referees, particularly by one of them, in evaluating the previous versions of the manuscript. Their suggestions and comments have greatly contributed to the improvement of this work. This work was funded by research Grants from Spanish MICINN. Ref. No. BIO2008-04500-C02-02 and from Canary Island Agency for Research PIL2070901 and PIL2071001.

## References

- [1] Kubicek, C. P., Zehentgruber, O., Rohr, M., An indirect method for studying the fine control of citric acid formation by *Aspergillus niger*. *Biotechnology Letters*\_1 (1979) 47-52.
- [2] Wolschek, M. F., Kubicek, C. P., The filamentous fungus *Aspergillus niger* contains two "differentially regulated" trehalose-6-phosphate synthase-encoding genes, *tpsA* and *tpsB*. *J Biol Chem* 272 (1997) 2729-2735.
- [3] Kubicek, C. P., The role of the citric acid cycle in fungal organic acid fermentations. *Biochem Soc Symp* 54 (1987) 113-126.

- [4] Roehr, M., Kubicek, C. P., Kominek, J., Industrial acids and other small molecules. *Biotechnology* 23 (1992) 91-131.
- [5] Karaffa, L., Kubicek, C. P., *Aspergillus niger* citric acid accumulation: do we understand this well working black box? *Appl Microbiol Biotechnol* 61 (2003) 189-196.
- [6] Legisa, M., Matthey, M., Changes in primary metabolism leading to citric acid overflow in *Aspergillus niger*. *Biotechnol Lett* 29 (2007) 181-190.
- [7] Papagianni, M., Advances in citric acid fermentation by *Aspergillus niger*: biochemical aspects, membrane transport and modeling. *Biotechnol Adv* 25 (2007) 244-263.
- [8] Torres, N. V., Modelling approach to control of carbohydrate metabolism during citric acid accumulation by *Aspergillus niger*. I. Model definition and stability of the steady state. *Biotechnol Bioeng* 44 (1994a) 104-111.
- [9] Torres, N. V., Modelling approach to control of carbohydrate metabolism during citric acid accumulation by *Aspergillus niger*. II. Sensitivity analysis. *Biotechnol Bioeng* 44 (1994b) 112-118.
- [10] Alvarez-Vasquez, F., Gonzalez-Alcon, C., Torres, N. V., Metabolism of citric acid production by *Aspergillus niger*: model definition, steady-state analysis and constrained optimization of citric acid production rate. *Biotechnol Bioeng* 70 (2000) 82-108.
- [11] Torres, N. V., Voit, E. O., González-Alcón, C., Rodríguez, F., A novel approach to design an overexpression strategy for metabolic engineering. Application to the carbohydrate metabolism in the citric acid producing mould *Aspergillus niger*. *Food Technology and Biotechnology* 36 (1998) 177-1184.
- [12] Guebel, D. V., Torres, N. V., Optimization of the citric acid production by *Aspergillus niger* through a metabolic flux balance model. *EJB Electronic Journal of Biotechnology* 4 (2001).
- [13] Torres, N., Riol-Cimas, J. M., Wolschek, M., Kubicek, C. P., Glucose transport by *Aspergillus niger*: the low affinity carrier is only formed during growth on high glucose concentrations. *Appl Microbiol Biotechnol* (1996).
- [14] Netik, A., Torres, N. V., Riol, J. M., Kubicek, C. P., Uptake and export of citric acid by *Aspergillus niger* is reciprocally regulated by manganese ions. *Biochim Biophys Acta* 1326 (1997) 287-294.
- [15] Peksel, A., Torres, N. V., Liu, J., Juneau, G., Kubicek, C. P., <sup>13</sup>C-NMR analysis of glucose metabolism during citric acid production by *Aspergillus niger*. *Appl Microbiol Biotechnol* 58 (2002) 157-163.
- [16] Ruijter, G. J., Panneman, H., van den Broeck, H. C., Bennett, J. M., Visser, J., Characterisation of the *Aspergillus nidulans* frA1 mutant: hexose phosphorylation and apparent lack of involvement of hexokinase in glucose repression. *FEMS Microbiol Lett* 139 (1996) 223-228.
- [17] Panneman, H., Ruijter, G. J., van den Broeck, H. C., Driever, E. T., Visser, J., Cloning and biochemical characterization of an *Aspergillus niger* glucokinase. Evidence for the presence of separate glucokinase and hexokinase enzymes. *Eur J Biochem* 240 (1996) 518-525.
- [18] Panneman, H., Ruijter, G. J., van den Broeck, H. C., Visser, J., Cloning and biochemical characterization of *Aspergillus niger* hexokinase--the enzyme is strongly inhibited by physiological concentrations of trehalose 6-phosphate. *Eur J Biochem* 258 (1998) 223-232.

- [19] Kubicek, C. P., Schrefel-Kunar, G., Wohrer, W., Rohr, M., Evidence for a cytoplasmic pathway of oxalate biosynthesis in *Aspergillus niger*. *Appl Environ Microbiol* 54 (1988) 633-637.
- [20] Burgstaller, W., Zanella, A., Schinner, F., Buffer-stimulated citrate efflux in *Penicillium simplicissimum*: an alternative charge balancing ion flow in case of reduced proton backflow? *Arch Microbiol* 161 (1994) 75-81.
- [21] Burgstaller, W., Thermodynamic boundary conditions suggest that a passive transport step suffices for citrate excretion in *Aspergillus* and *Penicillium*. *Microbiology* 152 (2006) 887-893.
- [22] Savageau, M. A., Biochemical systems analysis. I. Some mathematical properties of the rate law for the component enzymatic reactions. *J Theor Biol* 25 (1969a) 365-369.
- [23] Savageau, M. A., Biochemical systems analysis. II. The steady-state solutions for an n-pool system using a power-law approximation. *J Theor Biol* 25 (1969b) 370-379.
- [24] Voit, E. O., Computational Analysis of Biochemical System. A practical guide for biochemists and Molecular Biologists, Cambridge University Press, New York, 2000.
- [25] Savageau, M. A., Biochemical systems theory: operational differences among variant representations and their significance. *J Theor Biol* 151 (1991) 509-530.
- [26] Karaffa, L., Sandor, E., Fekete, E., Szentirmai, A., The biochemistry of citric acid accumulation by *Aspergillus niger*. *Acta Microbiol Immunol Hung* 48 (2001) 429-440.
- [27] Jernejc, K., Legisa, M., A drop of intracellular pH stimulates citric acid accumulation by some strains of *Aspergillus niger*. *J Biotechnol* 112 (2004) 289-297.
- [28] Hesse, S. J., Ruijter, G. J., Dijkema, C., Visser, J., Intracellular pH homeostasis in the filamentous fungus *Aspergillus niger*. *Eur J Biochem* 269 (2002) 3485-3494.
- [29] Sanders, D., Slayman, C. L., Control of intracellular pH. Predominant role of oxidative metabolism, not proton transport, in the eukaryotic microorganism *Neurospora*. *J Gen Physiol* 80 (1982) 377-402.
- [30] Papa, S., Lofrumento, N. E., Quagliariello, E., Meijer, A. J., Tager, J. M., Coupling mechanisms in anionic substrate transport across the inner membrane of rat-liver mitochondria. *J Bioenerg* 1 (1971) 287-307.
- [31] Konings, W. N., Poolman, B., Driessen, A. J., Can the excretion of metabolites by bacteria be manipulated? *FEMS Microbiol Rev* 8 (1992) 93-108.
- [32] Cassio, F., Leao, C., Low- and high-affinity transport systems for citric acid in the yeast *Candida utilis*. *Appl Environ Microbiol* 57 (1991) 3623-3628.
- [33] Corte-Real, M., Leao, C., Transport of malic acid and other dicarboxylic acids in the yeast *Hansenula anomala*. *Appl Environ Microbiol* 56 (1990) 1109-1113.
- [34] Cassio, F., Leao, C., van Uden, N., Transport of lactate and other short-chain monocarboxylates in the yeast *Saccharomyces cerevisiae*. *Appl Environ Microbiol* 53 (1987) 509-513.
- [35] Papagianni, M., Matthey, M., Kristiansen, B., The influence of glucose concentration on citric acid production and morphology of *Aspergillus niger* in batch and fed-batch culture. *Enzyme Microb Technol* 25 (1999) 710-717.

- [36] Wayman, F. M., Matthey, M., Simple diffusion is the primary mechanism for glucose uptake during the production phase of the *Aspergillus niger* citric acid process. *Biotechnol Bioeng* 67 (2000) 451-456.
- [37] Mark, C. G., Romano, A. H., Properties of the hexose transport systems of *Aspergillus nidulans*. *Biochim Biophys Acta* 249 (1971) 216-226.
- [38] Kumar, S., Punekar, N. S., SatyaNarayan, V., Venkatesh, K. V., Metabolic fate of glutamate and evaluation of flux through the 4-aminobutyrate (GABA) shunt in *Aspergillus niger*. *Biotechnol Bioeng* 67 (2000) 575-584.
- [39] Shen, W., Wei, Y., Dauk, M., Tan, Y., Taylor, D. C., Selvaraj, G., Zou, J., Involvement of a glycerol-3-phosphate dehydrogenase in modulating the NADH/NAD<sup>+</sup> ratio provides evidence of a mitochondrial glycerol-3-phosphate shuttle in *Arabidopsis*. *Plant Cell* 18 (2006) 422-441.
- [40] Teusink, B., Passarge, J., Reijenga, C. A., Esgalhado, E., van der Weijden, C. C., Schepper, M., Walsh, M. C., Bakker, B. M., van Dam, K., Westerhoff, H. V., Snoep, J. L., Can yeast glycolysis be understood in terms of in vitro kinetics of the constituent enzymes? Testing biochemistry. *Eur J Biochem* 267 (2000) 5313-5329.
- [41] Jennings, D. H., Polyol metabolism in fungi. *Adv Microb Physiol* 25 (1984) 149-193.
- [42] Mc, D. M., Martin, S. M., The hexosemonophosphate pathway in *Aspergillus niger*. *Can J Microbiol* 4 (1958) 329-333.
- [43] Habison, A., Kubicek, C. P., Rohr, M., Partial purification and regulatory properties of phosphofructokinase from *Aspergillus niger*. *Biochem J* 209 (1983) 669-676.
- [44] Kubicek-Pranz, E. M., Mozelt, M., Rohr, M., Kubicek, C. P., Changes in the concentration of fructose 2,6-bisphosphate in *Aspergillus niger* during stimulation of acidogenesis by elevated sucrose concentration. *Biochim Biophys Acta* 1033 (1990) 250-255.
- [45] Reich, J., Selkov, E., Energy metabolism of the cell, London Academic Press, London, 1981.
- [46] Kubicek, C. P., Röhr, M., The role of the tricarboxylic acid cycle in citric acid accumulation by *Aspergillus niger*. *Eur J Appl Microbiol Biotechnol* 5 (1978) 263-271.
- [47] Szutowicz, A., Bielarczyk, H., Elimination of CoASH interference from Acetyl-CoA cycling assay by maleic anhydride. *Anal Biochem* 164 (1987) 292-296.
- [48] Meixner-Monori, B., Kubicek, C. P., Harrer, W., Schrefel, G., Rohr, M., NADP-specific isocitrate dehydrogenase from the citric acid-accumulating fungus *Aspergillus niger*. *Biochem J* 236 (1986) 549-557.
- [49] Ruijter, G. J., Panneman, H., van den Broeck, H. C., Bennett, J. M., Visser, J., Characterisation of the *Aspergillus nidulans* frA1 mutant: hexose phosphorylation and apparent lack of involvement of hexokinase in glucose repression. *FEMS Microbiol Lett* 139 (1996) 223-228.
- [50] Fuhrer, L., Kubicek, C. P., Rohr, M., Pyridine nucleotide levels and ratios in *Aspergillus niger*. *Can J Biochem* 26 (1980) 405-408.
- [51] Arisan-Atac, I., Kubicek, C. P., Glycerol is not an inhibitor of mitochondrial citrate oxidation by *Aspergillus niger*. *Microbiology* 142 (Pt 10) (1996) 2937-2942.

- [52] Hesse, S. J., Ruijter, G. J., Dijkema, C., Visser, J., Measurement of intracellular (compartmental) pH by  $^31\text{P}$  NMR in *Aspergillus niger*. *J Biotechnol* 77 (2000) 5-15.
- [53] Garrib, A., McMurray, W. C., Purification and characterization of glycerol-3-phosphate dehydrogenase (flavin-linked) from rat liver mitochondria. *J Biol Chem* 261 (1986) 8042-8048.
- [54] Waddell, W. J., Ullberg, S., Marlowe, C., Localization of the bicarbonate and carbonate pools by whole-body autoradiography. *Arch Int Physiol Biochim* 77 (1969) 1-9.
- [55] Ferreira, A., Power Law Analysis and Simulation (PLAS), 2005.  
<http://www.dqb.fc.ul.pt/docentes/aferreira/plas.html>.
- [56] Serrano, R., Structure and function of proton translocating ATPase in plasma membranes of plants and fungi. *Biochim Biophys Acta* 947 (1988) 1-28.
- [57] Papagianni, M., Matthey, M., Morphological development of *Aspergillus niger* in submerged citric acid fermentation as a function of the spore inoculum level. Application of neural network and cluster analysis for characterization of mycelial morphology. *Microb Cell Fact* 5 (2006) 3.
- [58] Rohr, M., Kubicek, C. P., Zehentgruber, O., Orthofer, R., Accumulation and partial re-consumption of polyols during citric acid fermentation by *Aspergillus niger*. *Applied Microbiology and Biotechnology* 27 (1987) 47-52.
- [59] Paul, G. C., Priede, M. A., Thomas, C. R., Relationship between morphology and citric acid production in submerged *Aspergillus niger* fermentations. *Biochemical Engineering Journal* 3 (1999) 121-129.
- [60] Kubicek, C. P., Zehentgruber, O., El-Kalak, H., Rohr, M., Regulation of citric acid production by oxygen: effects of dissolved oxygen tension on adenylate levels and respiration in *Aspergillus niger*. *Eur J Appl Microbiol Biotechnol* 9 (1980) 101-116.
- [61] Promper, C., Schneider, R., Weiss, H., The role of the proton-pumping and alternative respiratory chain NADH:ubiquinone oxidoreductases in overflow catabolism of *Aspergillus niger*. *Eur J Biochem* 216 (1993) 223-230.
- [63] Bisaccia, F., De Palma, A., Dierks, T., Kramer, R., Palmieri, F., Reaction mechanism of the reconstituted tricarboxylate carrier from rat liver mitochondria. *Biochim Biophys Acta* 1142 (1993) 139-145.
- [64] de Jongh, W. A., Nielsen, J., Enhanced citrate production through gene insertion in *Aspergillus niger*. *Metab Eng* 10 (2008) 87-96.
- [65] Yan, F., Zhu, Y., Muller, C., Zorb, C., Schubert, S., Adaptation of  $\text{H}^+$ -pumping and plasma membrane  $\text{H}^+$  ATPase activity in proteoid roots of white lupin under phosphate deficiency. *Plant Physiol* 129 (2002) 50-63.
- [66] Evans, C. T., Scragg, A. H., Ratledge, C., A comparative study of citrate efflux from mitochondria of oleaginous and non-oleaginous yeasts. *Eur J Biochem* 130 (1983) 195-204.
- [67] Ten Brink, B., Konings, W. N., Generation of an electrochemical proton gradient by lactate efflux in membrane vesicles of *Escherichia coli*. *Eur J Biochem* 111 (1980) 59-66.

- [68] Guynn, R. W., Gelberg, H. J., Veech, R. L., Equilibrium constants of the malate dehydrogenase, citrate synthase, citrate lyase, and acetyl coenzyme A hydrolysis reactions under physiological conditions. *J Biol Chem* 248 (1973) 6957-6965.
- [69] Torres, N. V., Voit, E. O., *Pathways Analysis and Optimization in Metabolic Engineering*, Cambridge University Press, New York, 2002.
- [70] Vera, J., Torres, N. V., MetMAP: an integrated Matlab package for analysis and optimization of metabolic systems. *In Silico Biol* 4 (2004) 97-108.
- [71] Marín-Sanguino, A., Voit, E. O., Gonzalez-Alcon, C., Torres, N. V., Optimization of biotechnological systems through geometric programming. *Theor Biol Med Model* 4 (2007) 38.
- [72] Chou, I., Voit, E.O. Recent developments in parameter estimation and structure identification of biochemical and genomics systems. *Mathem. Biosc.* 219 (2009) 57-83.
- [73] Kirimura, K., Yoda, M., Shimizu, H., Sugano, S., Mizuno, M., Kino, K. and Usammi, S. Contribution of cyanide-insensitive respiratory pathway, catalyzed by the alternative oxidase, to citric acid production in *Aspergillus niger*. *Biosci Biotechnol. Biochem.* 64(10) (2000). 2034-2039.

**Mathematical modelling and assessment of the pH homeostasis mechanisms in *Aspergillus niger* while in citric acid producing conditions.**

**Supplementary section**

**Equations S1. S-system model with numerical values**

$$\frac{dX_1}{dt} = .002697 X_{78}^{.03670} X_{66}^{1.000} X_{33}^1 - 47.88 X_1^{.9915} X_{28}^{.2106} X_{34}^1.$$

$$\frac{dX_2}{dt} = 14.87 \frac{X_1^{.3391} X_{28}^{.07205} X_{34}^{.3421} X_{36}^{.6579} X_3^{1.711}}{X_2^{.5168}} - .06590 \frac{X_{36}^{.9404} X_2^{1.480} X_{58}^{.05970}}{X_3^{.02660}}$$

$$\frac{dX_3}{dt} = 2.478 \frac{X_{28}^{.07559} X_{19}^{.3587} X_{34}^{.3593} X_{36}^{.5136} X_2^{.7976} X_{37}^{.1271} X_4^{.1060}}{X_3^{.01452}} - 28.75 \frac{X_{36}^{.3593} X_3^{1.255} X_{18}^{.001080} X_{60}^{.1374} X_{38}^{.3404} X_{28}^{.007355} X_{39}^{.6407}}{X_2^{.2822}}$$

$$\frac{dX_4}{dt} = 19.24 \frac{X_3^{.4999} X_{60}^{.2145} X_{38}^{.5312} X_{28}^{.01148} X_{39}^1}{X_{18}^{.6163}} - 2.789 X_{37}^{.1984} X_4^{.9553} X_{56}^{.8015}$$

$$\frac{dX_5}{dt} = .05963 X_4^{.2380} X_{56}^{.2476} X_{20}^{.7121} X_{55}^{.7524} - .8110 \frac{X_{22}^{1.012} X_5^{.5721} X_{40}^1 X_{71}^{.2846}}{X_{28}^{.01101}}$$

$$\frac{dX_6}{dt} = .8690 X_{72}^{.4034} X_{22}^{1.005} X_5^{.5679} X_{40}^{.9929} X_{28}^{.003296} X_{71}^{.2898} X_8^{.005920} X_6^{.008274} X_{35}^{.007103} - 16.20 \frac{X_6^{.9924} X_{35}^{.007103} X_{71}^{.08629} X_{41}^{.9929}}{X_8^{.00008339} X_{28}^{.003188}}$$

$$\frac{dX_7}{dt} = 16.11 \frac{X_{41}^1 X_6^{.9853} X_{71}^{.07826}}{X_{28}^{.01788}} - 6.810 X_7^{.7697} X_{28}^{.06132} X_{42}^{.7524} X_{45}^{.2476}$$

$$\frac{dX_8}{dt} = .9980 \frac{X_6^{.01418} X_{28}^{.07556} X_{35}^{.007113} X_{71}^{.008584} X_7^{.5238} X_{42}^{.7481} X_9^{.2531} X_{43}^{.2447}}{X_8^{.00008842} X_{22}^{.00004197} X_{72}^{.00002325}} - .00002364 \frac{X_{43}^{.9789} X_9^{.9818} X_8^{.9901} X_{28}^{.01425} X_6^{.008286} X_{35}^{.007113} X_{71}^{.007182} X_{44}^{.01403}}{X_{22}^{3.548}}$$

$$\frac{dX_9}{dt} = .00001540 \frac{X_{43}^1 X_9^{1.003} X_8^{.9913}}{X_{22}^{3.625} X_{72}^{.7418}} - .2156 \frac{X_9^{1.075} X_{15}^{.0007365} X_{64}^{.7500} X_{43}^{.2500}}{X_8^{.5018} 10^{-5} X_{22}^{.00004288}}$$

$$\frac{dX_{10}}{dt} = 1.269 X_9^{.8159} X_{15}^{.0007365} X_{64}^{.7500} X_{72}^{.2585} X_{30}^{.4872} X_{11}^{.2431} X_{10}^{.2505} X_{48}^{.2500} - .0002312 \frac{X_{72}^1 X_{10}^{1.007} X_{48}^1}{X_{30}^{.001056} X_{11}^{.00001405}}$$

$$\frac{dX_{11}}{dt} = .0002312 \frac{X_{72}^1 X_{10}^{1.007} X_{48}^1}{X_{30}^{.001056} X_{11}^{.00001405}} - 660.8 X_{11}^{.8136} X_{14}^{.4035} X_{47}^{.7500} X_{72}^{.2585} X_{30}^{.4872} X_{10}^{.2505} X_{48}^{.2500}$$

$$\frac{dX_{12}}{dt} = 306.8 X_{14}^{.5382} X_{47}^1 - 1.104 X_{46}^1 X_{12}^{.08429}$$

$$\frac{dX_{13}}{dt} = 198.0 X_{45}^{.2511} X_7^{.2463} X_{17}^{.5880} X_{53}^{.7489} - .1850 \frac{X_{46}^{.7489} X_{12}^{.06314} X_{13}^{.2431} X_{72}^{.08509} X_{53}^{.2511}}{X_{30}^{.8738}}$$

$$\frac{dX_{14}}{dt} = 1.019 \frac{X_{46}^{1.000} X_{12}^{.08430} X_{13}^{.001649} X_{72}^{.01064}}{X_{30}^{.1092}} - 353.2 X_{12}^{.01932} X_{14}^{.5383} X_{47}^{1.000}$$

$$\frac{dX_{15}}{dt} = 809.6 X_{11}^{.3800} X_{14}^{.5374} X_{47}^{.9990} X_{15}^{.0009854} X_{16}^{.0008975} X_{49}^{.0009737} X_{12}^{.1030} \\ - .02422 \frac{X_{49}^{.4995} X_{15}^{1.344} X_{64}^{.5005} X_9^{.04401}}{X_{16}^{.01392}}$$

$$\frac{dX_{16}}{dt} = .002280 \frac{X_{49}^{.9981} X_{15}^{1.685} X_{76}^{.001946} X_{30}^{.01158} X_{17}^{.0002611} X_{72}^{.002936}}{X_{16}^{.02440}} \\ - .9070 \frac{X_{16}^{1.208} X_{76}^{.9981} X_{72}^{.9981} X_{15}^{.001969} X_{49}^{.001946}}{X_{30}^{.02220} X_{17}^{.002547}}$$

$$\frac{dX_{17}}{dt} = 3.618 \frac{X_{16}^{.9047} X_{76}^{.7489} X_{72}^{.7489} X_{13}^{.2299} X_{53}^{.2511}}{X_{30}^{.01666} X_{17}^{.001911}} \\ - 106.9 X_{17}^{.7130} X_{50}^{.2496} X_{76}^{.001460} X_{30}^{.008684} X_{72}^{.002203} X_{16}^{.002558} X_{53}^{.7489}$$

$$\frac{dX_{18}}{dt} = 10.43 X_{15}^{.5005} X_{64}^{.5000} X_9^{.04397} X_{73}^{.5000} X_{29}^{.5000} X_{18}^{.5000} - .7762 \frac{X_{73}^{.5000} X_{61}^{.5000} X_{18}^{.3351}}{X_{29}^{.00001256}}$$

$$\frac{dX_{19}}{dt} = .02460 X_{59}^1 X_{32}^{.005420} - 75.10 X_{28}^{.2104} X_{19}^{.9984} X_{34}^1$$

$$\frac{dX_{20}}{dt} = 1.719 X_4^{.9086} X_{56}^{.9147} X_{67}^{.08548} - .03009 X_{20}^{.9357} X_{55}^{.9147} X_{54}^{.08548} X_{22}^{.06837}$$

$$\frac{dX_{21}}{dt} = 6.099 X_{54}^1 X_{20}^{.8192} X_{22}^{.8001} - .008496 X_{21}^1$$

$$\frac{dX_{22}}{dt} = 1.047 \frac{X_9^{.007308} X_{22}^{.02906} X_{43}^{.007067} X_{72}^{.01166} X_5^{.01643} X_{40}^{.02871} X_{71}^{.008173} X_{70}^{.9643}}{X_8^{.1419 \cdot 10^{-6}} X_{28}^{.0003161}} - 20.57 X_{22}^{.8687} X_{54}^{.002019} X_{20}^{.001654} X_{43}^{.02826} X_9^{.02835} X_8^{.02802}$$

$$\frac{dX_{23}}{dt} = .008496 X_{21}^1 - 47.84 X_{31}^{2.221} X_{68}^1 X_{67}^{1.966} X_{23}^{.9945}$$

$$\frac{dX_{24}}{dt} = .04627 X_{17}^{.2500} X_{50}^{.5000} X_{65}^{.5000} X_{74}^{.02469} X_{26}^{.04336} - .007948 X_{57}^{.5000} X_{24}^{.1922} X_{62}^{.5000}$$

$$\frac{dX_{25}}{dt} = .001906 X_{57}^1 X_{24}^{.3689} - .01458 X_{65}^1 X_{25}^{.3817}$$

$$\frac{dX_{26}}{dt} = .08959 \frac{X_{77}^{.5000} X_{74}^{.5000} X_{62}^{.5000} X_{24}^{.007763}}{X_{26}^{.5000}} - .0003417 X_{26}^1 X_{74}^1$$

$$\frac{dX_{27}}{dt} = 31.45 X_{29}^1 X_{75}^1 X_{27}^1 - .0007900 X_{75}^1 X_{27}^1$$

$$\frac{dX_{28}}{dt} = .2422 \frac{X_6^{.02384} X_{28}^{.8659} X_{35}^{.0001706} X_{71}^{.008864} X_{69}^{.9519} X_{41}^{.02385} X_{72}^{.009690} X_{22}^{.02414} X_5^{.01364} X_{40}^{.02385}}{X_8^{.2003 \cdot 10^{-5}}} - .1221 X_1^{.008601} X_{28}^{1.984} X_{34}^{.02537} X_{18}^{.00005015} X_3^{.01488} X_{60}^{.006384} X_{38}^{.01581} X_{39}^{.02976} X_7^{.01257} X_{42}^{.01795} X_{69}^{.9185} X_{19}^{.01666} X_{29}^{.004102} X_{63}^{.008208} X_8^{.0001422} X_6^{.0001988} X_{35}^{.0001706} X_{71}^{.0001723}$$

$$\frac{dX_{29}}{dt} = .1565 X_{57}^{.7875e-1} X_{24}^{.2905e-1} X_{73}^{.2367} X_{77}^{.4268} X_{75}^{.2590} X_{27}^{.2590} - 123.6 X_{73}^{.2367} X_{29}^{.5507} X_{18}^{.3953} X_{75}^{.2590} X_{61}^{.2367} X_{28}^{.2597e-1} X_{63}^{.1101} X_{62}^{.7875e-1} X_{24}^{.1223e-2} X_{65}^{.7875e-1} X_{25}^{.3006e-1} / X_{27}^{.2590}$$

$$\frac{dX_{30}}{dt} = .05409 X_{72}^{.6944} X_{10}^{.3811} X_{48}^{.3784} X_{46}^{.2838} X_{12}^{.02393} X_{13}^{.004996} X_{16}^{.3429} X_{76}^{.2838} X_{54}^{.02703} X_{20}^{.02214} X_{22}^{.02162} X_{31}^{.06003} X_{68}^{.02703} X_{67}^{.05314} X_{23}^{.02687} / \left( X_{30}^{.3377} X_{11}^{.5317} 10^{-5} X_{17}^{.0007243} \right) - 4.553 X_{52}^{.8779} X_{51}^{.8779} X_{30}^{.1964} X_{72}^{.1026} X_{11}^{.09199} X_{10}^{.09480} X_{48}^{.09461} X_{76}^{.0005533} X_{17}^{.00007425} X_{16}^{.0009693} X_{67}^{.04748} X_{31}^{.03281} X_{68}^{.02703}$$

$$\frac{dX_{31}}{dt} = 47.84 X_{31}^{2.221} X_{68}^1 X_{67}^{1.966} X_{23}^{.9945} - .3899 X_{67}^{1.757} X_{31}^{1.214} X_{68}^1$$

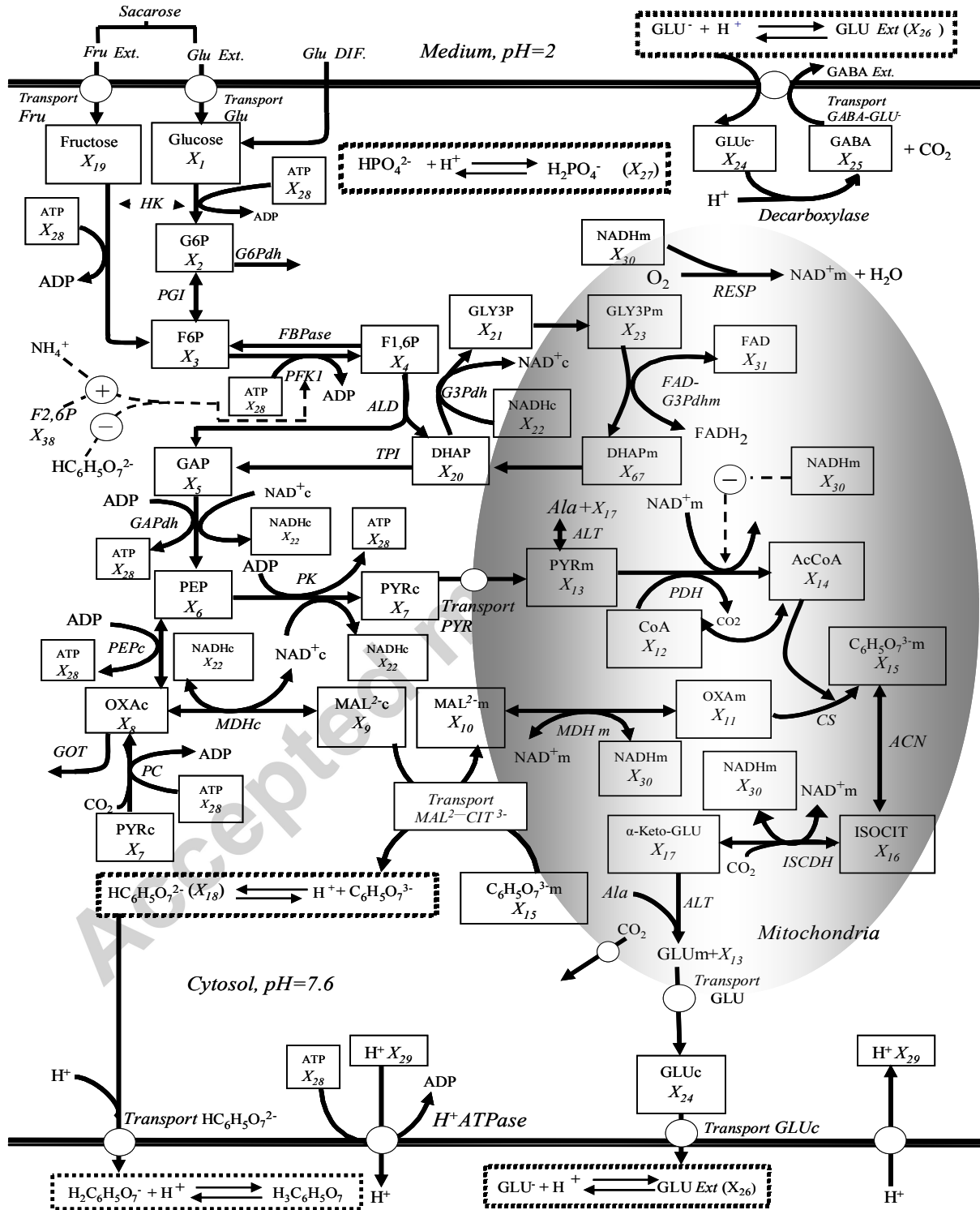
Accepted manuscript

Table S1. Basal, steady state eigenvalues in *A. niger* while in citric acid producing conditions

| min <sup>-1</sup>           |                                |
|-----------------------------|--------------------------------|
| -1904                       | -0.09807                       |
| -39.64                      | -0.05216                       |
| -31.28                      | -0.009202+ 0.01143 <i>i</i>    |
| -10.25                      | -0.009202- 0.01143 <i>i</i>    |
| -9.838                      | -0.01885                       |
| -5.547                      | -0.01885                       |
| -3.659                      | -0.008485                      |
| -3.309                      | -0.004328+ 0.002277 <i>i</i>   |
| -2.752                      | -0.004328- 0.002277 <i>i</i>   |
| -1.573                      | -0.0006934+ 7.944 E-5 <i>i</i> |
| -0.5001                     | -0.0006934- 7.944 E-5 <i>i</i> |
| -0.4994                     | -0.002239                      |
| -0.1864                     | -0.002239                      |
| -0.1646                     | -0.005449                      |
| -0.1270                     |                                |
| -0.1073+ 0.008618 <i>i</i>  |                                |
| -0.1073 - 0.008618 <i>i</i> |                                |

Accepted manuscript

Figure 1



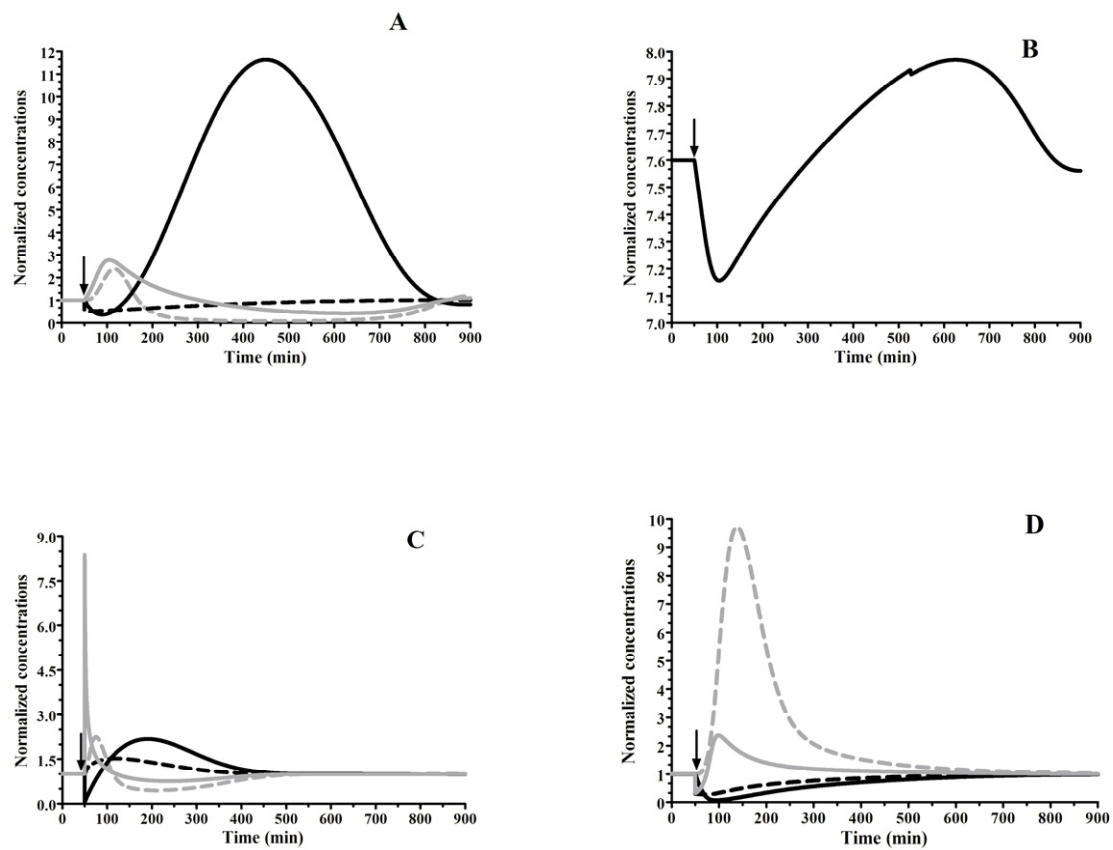


Figure 2

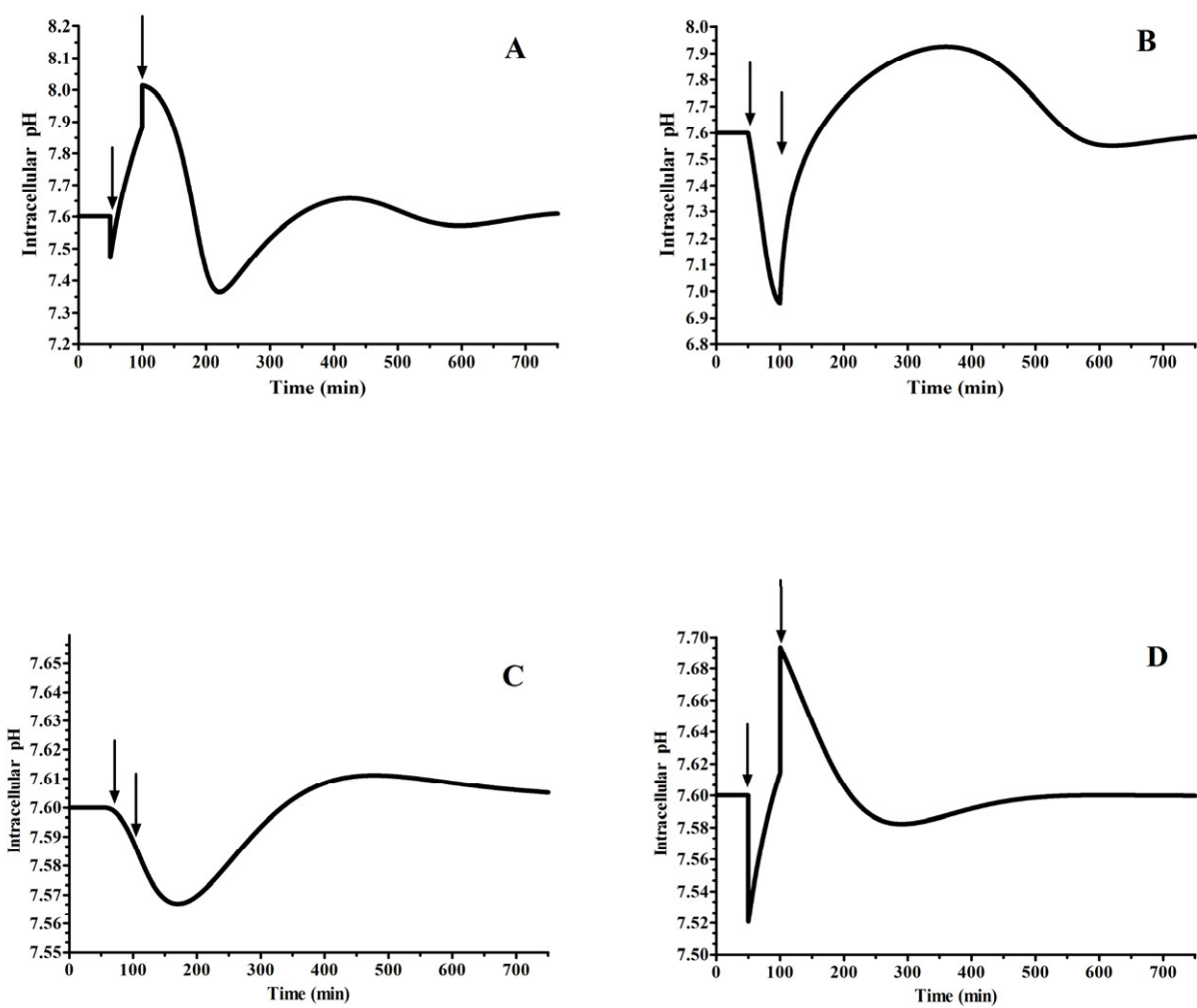


Figure 3

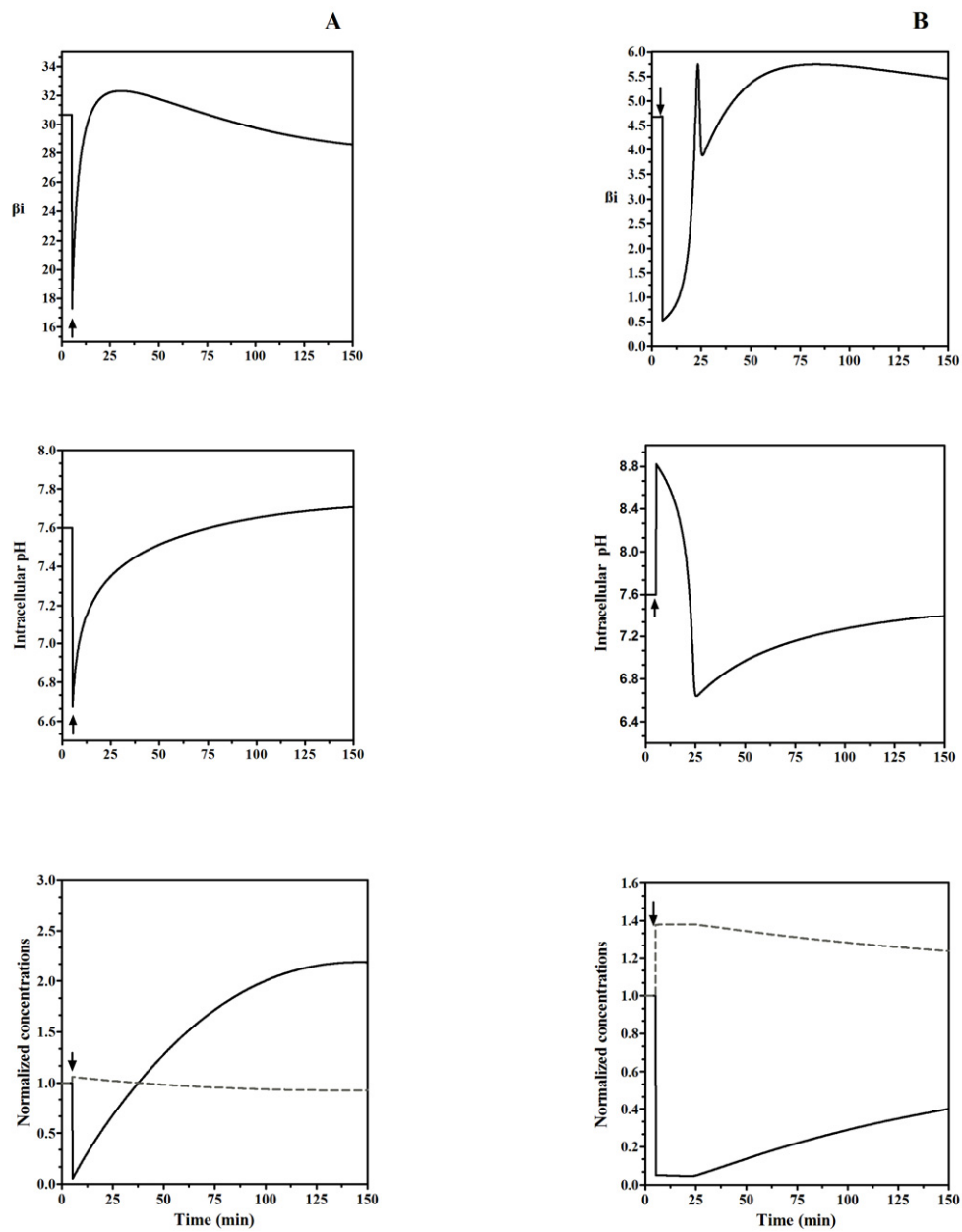


Figure 4

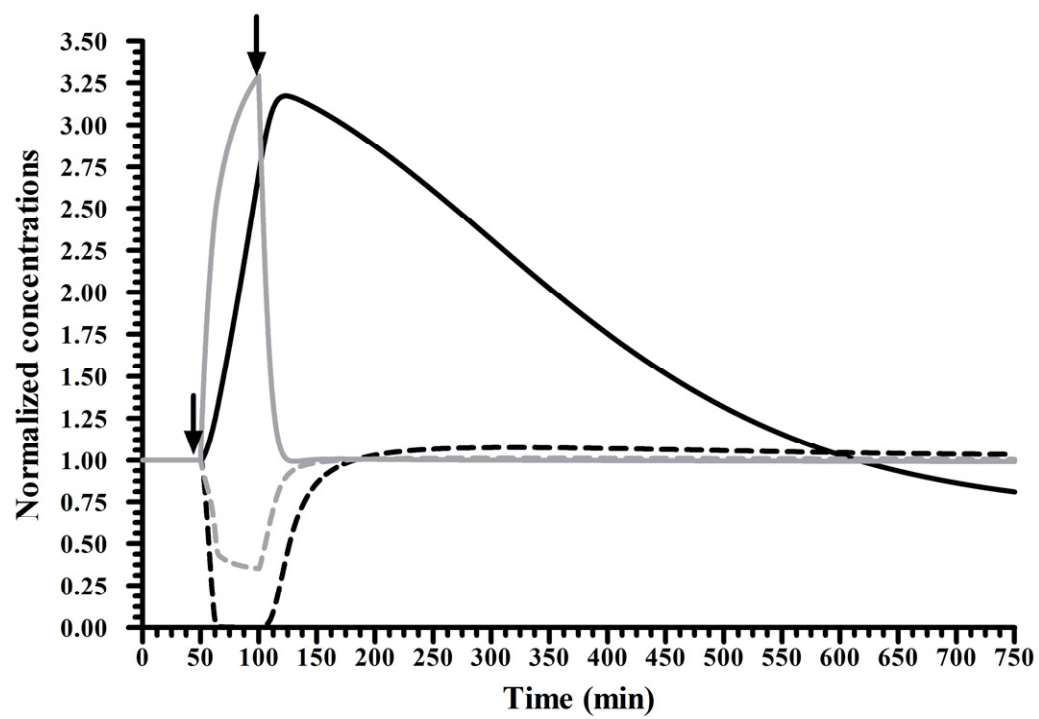


Figure 5

Accepted ma

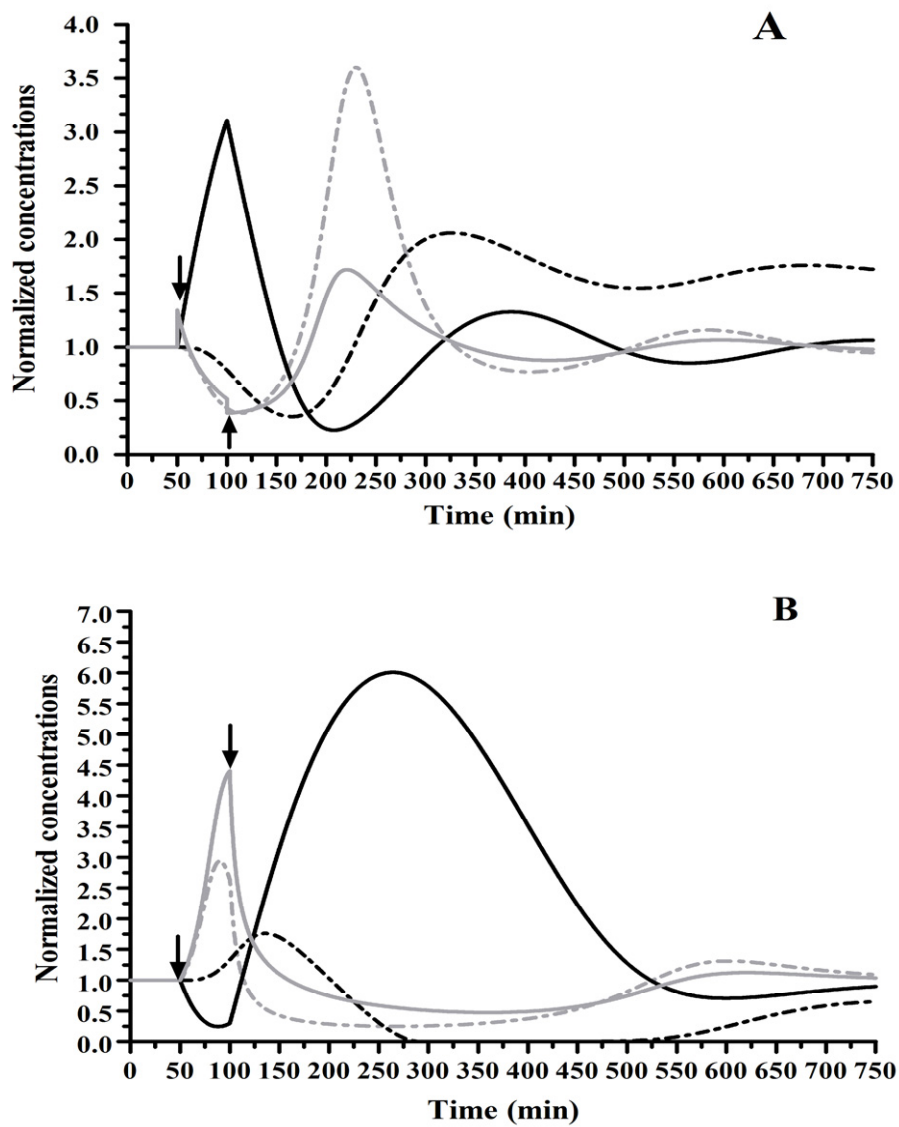


Figure 6

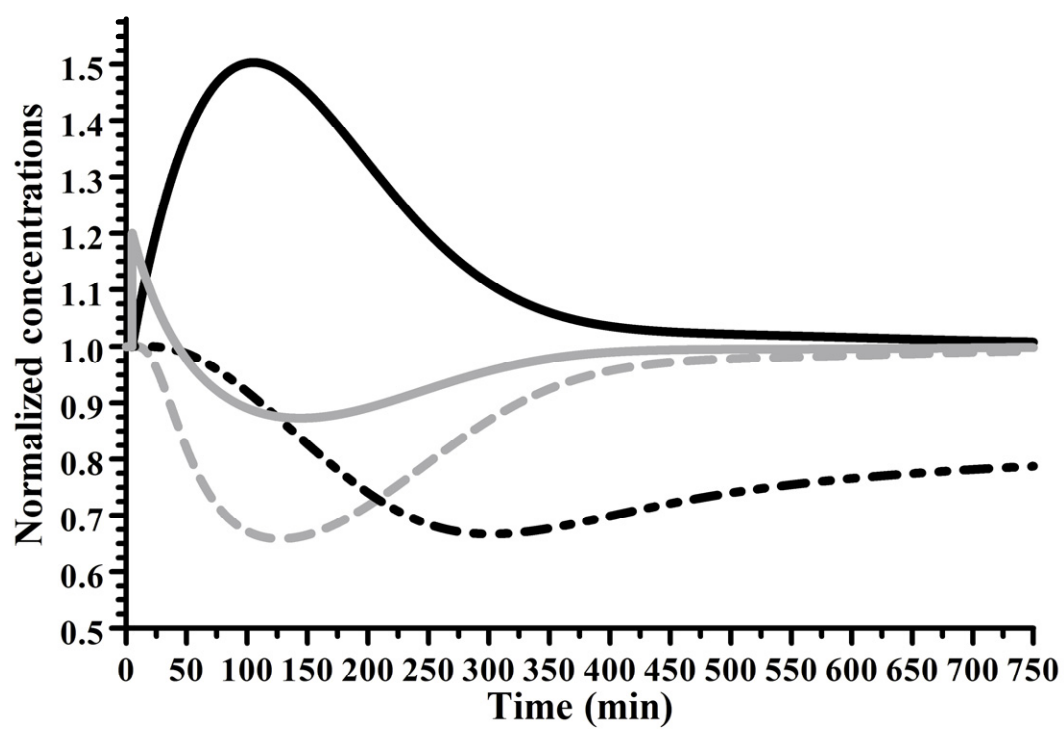


Figure 7

Accepted ma

**Figure 1. Metabolic network of the main metabolic pathways involved in citric acid synthesis and pH homeostasis in *A. niger* while in citric acid producing conditions.** Metabolites are shown in boxes and reactions are indicated by arrows. Lines indicate reactions or transport processes, whereas dotted lines indicate regulatory interactions or buffers. Solid dots represent transport systems. Dependent variables are numbered from 1 to 31: Glucose ( $X_1$ , cytoplasmic glucose); G6P ( $X_2$ , glucose-6-phosphate); F6P ( $X_3$ , fructose-6-phosphate); F1,6P ( $X_4$ , fructose 1,6 biphosphate); GAP ( $X_5$ , glyceraldehyde-3-phosphate); PEP ( $X_6$ , phosphoenol pyruvate); PYRc ( $X_7$ , cytoplasmic pyruvate); OXAc ( $X_8$ , cytoplasmic oxaloacetate); MAL<sup>2-c</sup> ( $X_9$ , cytoplasmic malate); MAL<sup>2-m</sup> ( $X_{10}$ , mitochondrial malate); OXAm ( $X_{11}$ , mitochondrial oxaloacetate); CoA ( $X_{12}$ , CoA); PYRm ( $X_{13}$ , mitochondrial pyruvate); AcCoA, ( $X_{14}$ , acetyl-CoA); C<sub>6</sub>H<sub>5</sub>O<sub>7</sub><sup>3-m</sup> ( $X_{15}$ , mitochondrial citrate); ISC ( $X_{16}$ , isocitrate);  $\alpha$ -Keto-GLU ( $X_{17}$ ,  $\alpha$ -keto-glutarate mitochondrial); HC<sub>6</sub>H<sub>5</sub>O<sub>7</sub><sup>2</sup> ( $X_{18}$ , cytoplasmic citrate, reduced form); Fructose. ( $X_{19}$ , cytoplasmic fructose); DHAP ( $X_{20}$ , cytoplasmic dihydroxyacetone phosphate); GLY3P ( $X_{21}$ , glycerol-3-phosphate); NADHc ( $X_{22}$ , cytoplasmic nicotinamide adenine dinucleotide); Glycerol ( $X_{23}$ , glycerol); GLUc ( $X_{24}$ , cytoplasmic glutamate); GABA ( $X_{25}$ , 4-aminobutyrate); GLUe ( $X_{26}$ , extracellular glutamate, reduced form); GLUe<sup>-</sup> ( $X_{26}$ , extracellular glutamate, anion form); H<sub>2</sub>PO<sub>4</sub><sup>-</sup> ( $X_{27}$ , cytoplasmic phosphate, reduced form); ATP ( $X_{28}$ , adenosine triphosphate); H<sup>+</sup> ( $X_{29}$ , intracellular protons); NADHm ( $X_{30}$ , mitochondrial nicotinamide adenine dinucleotide); FADH<sub>2</sub> ( $X_{31}$ , flavin adenine dinucleotide reduced form). Independent variables are numbered from 32 to 78: *Fru Ext.* ( $X_{32}$ , medium fructose); *Transport Glu* ( $X_{33}$ , glucose carrier); *HK* ( $X_{34}$ , hexokinase); *PEPc* ( $X_{35}$ , cytoplasmic phosphoenol pyruvate carboxykinase); *PGI* ( $X_{36}$ , phosphoglucose isomerase); *FBPase*, ( $X_{37}$ , fructose-2,6-bisphosphatase); F2,6P ( $X_{38}$ , fructose 2,6 biphosphate); *PFK1* ( $X_{39}$ , 6-phosphofructo-1-kinase); *GA3Pdh* ( $X_{40}$ , glyceraldehyde-3-phosphate dehydrogenase); *PK* ( $X_{41}$ , pyruvate kinase); *PC* ( $X_{42}$ , pyruvate carboxylase); *MDHc* ( $X_{43}$ , cytoplasmic malate dehydrogenase); *GOT* ( $X_{44}$ , aspartate aminotransferase); *Transport PYR* ( $X_{45}$ , mitochondrial pyruvate carrier system); *PDH* ( $X_{46}$ , pyruvate dehydrogenase); *CS* ( $X_{47}$ , citrate synthase); *MDHm* ( $X_{48}$ , mitochondrial malate dehydrogenase); *ACN* ( $X_{49}$ , aconitase); *Transport GLUm*, ( $X_{50}$ , mitochondrial glutamate transport); *RESP* ( $X_{51}$ , alternative respiratory system); O<sub>2</sub> ( $X_{52}$ , oxygen uptake); *ALT* ( $X_{53}$ , alanine transaminase); *G3Pdh* ( $X_{54}$ , glycerol-3-phosphate dehydrogenase); *TPI* ( $X_{55}$ , triose-phosphate-isomerase); *ALD* ( $X_{56}$ , fructose-biphosphate aldolase); *Decarboxylase* ( $X_{57}$ , glutamate decarboxylase); *G6Pdh* ( $X_{58}$ , glucose-6-phosphate dehydrogenase); *Transport Fru* ( $X_{59}$ , fructose carrier); NH<sub>4</sub><sup>+</sup> ( $X_{60}$ , ammonium); *Transport HC<sub>6</sub>H<sub>5</sub>O<sub>7</sub><sup>2-</sup>* ( $X_{61}$ , cytoplasmic dihydrogen citrate ion carrier); *Transport GLUc* ( $X_{62}$ , cytoplasmic glutamate carrier); *H<sup>+</sup>ATPase*, ( $X_{63}$ , *H<sup>+</sup>ATPase*); *Transport MAL<sup>2-</sup>-CIT<sup>3-</sup>*, ( $X_{64}$ , mitochondrial malate-hydrogen citrate ion antiporter carrier system); *Transport GABA-GLU* ( $X_{65}$ , GABA-glutamate carrier); *Glu DIF.* ( $X_{66}$ , glucose diffusion); *DHAPm* ( $X_{67}$ , mitochondrial dihydroxyacetone phosphate); FAD-G3P ( $X_{68}$ , FAD-glycerol-3-phosphate dehydrogenase); *AK* ( $X_{69}$ , adenylate kinase); *NADHase* ( $X_{70}$ , NADH dehydrogenase); *ATP Total* ( $X_{71}$ ); *NADH Total* ( $X_{72}$ ); Total citrate concentration ( $X_{73}$ ); Total glutamate concentration ( $X_{74}$ ); Total phosphate concentration ( $X_{75}$ ); *ISCDH* ( $X_{76}$ , isocitrate dehydrogenase); *External Protons* ( $X_{77}$ ); *Ala* (Alanine); *Glu Ext.* ( $X_{78}$ , medium glucose). See text for further explanations.

**Figure 2. System dynamic response against different pulse perturbations experiments in *A. niger* while in citric acid producing conditions.** At time 50 min. (arrow) the concentration of a dependent variable was momentarily decreased and the time evolution of the remaining metabolites concentration were monitored. **A.** Dynamics of cytoplasmic pyruvate ( $X_7$ ; grey dashed line);  $C_6H_5O_7^{3-m}$  ( $X_{15}$ ; black dashed line);  $HC_6H_5O_7^{2-}$  ( $X_{18}$ ; black solid line) and intracellular  $H^+$  ( $X_{29}$ ; grey solid line) after a 50% decrease in the mitochondrial citrate concentration ( $X_{15}$ ). **B.** Intracellular pH system dynamics after a 50% decrease in the mitochondrial citrate concentration ( $X_{15}$ ). **C.** Dynamics of  $X_7$  (grey dashed line);  $X_{18}$  (black solid line);  $X_{27}$  (black dashed line) and  $X_{29}$  (grey solid line) after a 95% decrease in the reduced cytoplasmic citrate ( $X_{18}$ ). **D.** Dynamics of  $X_7$  (grey dashed line);  $X_{18}$  (black solid line);  $X_{27}$  (black dashed line) and  $X_{29}$  (grey solid line) after a transitory 70% decrease in the reduced cytoplasmic phosphate ( $H_2PO_4^-$ ;  $X_{27}$ ). In all cases, only those variables showing significant changes are represented. Data are represented as normalized values with respect to the reference steady state.

**Figure 3. Dynamic response of the cytoplasmic pH to different parameter changes in *A. niger* while in citric acid producing conditions.** In all cases, starting from the citric acid producing steady state, the basal value of a parameter was kept constant from minute 50 until minute 100 at 40% (indicated by arrows) of its original value, and the time evolution of cytoplasmic pH was recorded. **A.** pH evolution after changing the cytoplasmic citrate carrier,  $X_{61}$ . **B.** pH evolution after changing the mitochondrial malate-citrate transport system  $X_{64}$ . **C.** pH evolution after changing of the alternative respiratory system,  $X_{51}$ . **D.** pH evolution after changing the  $H^+$ -ATPase,  $X_{63}$ .

**Figure 4. Dynamics of the cytoplasmic buffer capacity ( $\beta_i$ ) in *A. niger* while in citric acid producing conditions.** At time 5 min (arrow) the concentrations of  $HC_6H_5O_7^{2-}$ ,  $X_{18}$  (A) or  $H_2PO_4^-$ ,  $X_{27}$  (B) were decreased by a 95% of its steady state value and the evolution of the buffer capacity,  $\beta_i$ , intracellular pH and the buffer components were recorded. In A dashed lines represent the concentration of  $C_6H_5O_7^{3-}$  while in B dashed line represents the concentration of  $HPO_4^{2-}$ . In both cases the total concentration of the buffer pair was kept constant ( $X_{73}$  and  $X_{75}$ , respectively). Data are represented as normalized values with respect the reference steady state.

**Figure 5. Dynamic response after a transient perturbation in the alternative respiratory system in *A. niger* while in citric acid producing conditions.** In these experiments, starting from the citric acid producing steady state, the basal value of the alternative respiratory system,  $X_{51}$  was kept constant from minute 50 until minute 100 (arrows) at 60% of its original value. The evolution of those variables showing significant changes is represented: CoA ( $X_{12}$ ; black dashed line); mitochondrial pyruvate ( $X_{13}$ ; black solid line); acetyl-CoA ( $X_{14}$ ; grey dashed line); NADHm ( $X_{30}$ ; grey solid line). Data are represented as normalized values with respect the reference steady state.

**Figure 6. Dynamic response to transient perturbations in the cytoplasmic citrate carrier and mitochondrial malate-citrate transport system in *A. niger* while in citric acid producing conditions.** In these experiments, starting from the citric acid producing steady state, the basal values of two parameters were kept constant from minute 50 until minute 100 (arrows) at 60% of its original value and the time evolution of the variables showing significant changes were represented. **A.** Predicted changes after inhibition of the cytoplasmic citrate carrier,  $X_{61}$ : cytoplasmic pyruvate ( $X_7$ ; grey dashed line); mitochondrial pyruvate ( $X_{13}$ ; black dashed line);  $HC_6H_5O_7^{2-}$  ( $X_{18}$ ; black solid line) and intracellular  $H^+$  ( $X_{29}$ ; grey solid line). **B.** Predicted changes after inhibition of the mitochondrial malate-citrate transport system, ( $X_{64}$ ):  $X_7$  (grey dashed line);  $X_{13}$  (black dashed line);  $X_{18}$  (black solid line) and  $X_{29}$  (grey solid line). Data are represented as normalized values with respect the reference steady state.

**Figure 7. Dynamic response to transient perturbations in the  $H^+$ ATPase in *A. niger* while in citric acid producing conditions.** In these experiments, starting from the citric acid producing steady state  $X_{63}$  was kept

constant at a decreased 60% from its steady state value and the evolution of the whole system was recorded. PYRc ( $X_7$ ; grey dashed line);  $\alpha$ -KetoGLU ( $X_{17}$ ; black dashed line);  $\text{HC}_6\text{H}_5\text{O}_7^{2-}$  ( $X_{18}$ ; black solid line) and intracellular  $\text{H}^+$  ( $X_{29}$ ; grey solid line). There are only represented those variables showing significant changes.

Accepted manuscript

| Metabolite                                 | Abbreviation   | Variable (X <sub>i</sub> ) | Concentration (mM) | Flux (μmol/l <sub>t</sub> min) | Reference |
|--|--|----------------------------|--------------------|--------------------------------|-----------|
| Cytoplasmic Glucose                        | Glucose  | X <sub>1</sub>             | 0.0027             | 0.010                          | [42]      |
| Glucose-6-phosphate                        | G6P  | X <sub>2</sub>             | 0.1                | 0.029                          | [43]      |
| Fructose-6-phosphate                       | F6P  | X <sub>3</sub>             | 0.025              | 0.054                          | [43]      |
| Fructose 1,6 biphosphate                   | F1,6P  | X <sub>4</sub>             | 0.02               | 0.034                          | [44]      |
| Glyceraldehyde-3-phosphate                 | GAP  | X <sub>5</sub>             | 0.15               | 0.027                          | [40]      |
| Phosphoenol pyruvate                       | PEP  | X <sub>6</sub>             | 0.01               | 0.027                          | [45]      |
| Cytoplasmic pyruvate                       | PYRc   | X <sub>7</sub>             | 0.12               | 0.027                          | [44]      |
| Cytoplasmic oxaloacetate                   | OXA <sub>c</sub>   | X <sub>8</sub>             | 5.8e-4             | 0.027                          | [46]      |
| Cytoplasmic malate                         | MAL <sup>2-</sup> c  | X <sub>9</sub>             | 2.6                | 0.027                          | [46]      |
| Mitochondrial malate                       | MAL <sup>2-</sup> m  | X <sub>10</sub>            | 13                 | 0.027                          | [46]      |
| Mitochondrial oxaloacetate                 | OXA <sub>m</sub>   | X <sub>11</sub>            | 0.002              | 0.027                          | [46]      |
| CoA  | CoA  | X <sub>12</sub>            | 0.108              | 0.198                          | [47]      |
| Mitochondrial pyruvate                     | PYR <sub>m</sub>   | X <sub>13</sub>            | 0.56               | 0.027                          | [46]      |
| Acetyl-CoA                                 | AcCoA  | X <sub>14</sub>            | 0.012              | 0.219                          | [46]      |
| Mitochondrial citrate                      | C <sub>6</sub> H <sub>7</sub> O <sub>7</sub> <sup>3-</sup> m | X <sub>15</sub>            | 31.25              | 0.041                          | [48]      |
| Isocitrate                                 | ISC  | X <sub>16</sub>            | 1.21               | 0.020                          | [48]      |
| α-keto-glutarate mitochondrial             | α-KetoGLU  | X <sub>17</sub>            | 0.040              | 0.027                          | [48]      |
| Cytoplasmic citrate (divalent)             | HC <sub>6</sub> H <sub>7</sub> O <sub>7</sub> <sup>2-</sup>  | X <sub>18</sub>            | 0.333              | 0.041                          | Estimated |
| Cytoplasmic citrate (trivalent)            | C <sub>6</sub> H <sub>7</sub> O <sub>7</sub> <sup>3-</sup>   | --                         | 5.284              | --                             | Estimated |
| Cytoplasmic fructose                       | Fructose   | X <sub>19</sub>            | 0.0035             | 0.019                          | [42]      |
| Dihydroxyacetone phosphate                 | DHAP   | X <sub>20</sub>            | 0.17               | 0.022                          | [49]      |
| Glycerol-3-phosphate                       | GLY3P  | X <sub>21</sub>            | 0.23               | 0.002                          | [49]      |
| Nicotinamide adenine dinucleotide reduced  | NADH <sub>c</sub>  | X <sub>22</sub>            | 0.035              | 0.968                          | [50]      |
| Nicotinamide adenine dinucleotide oxidized | NAD <sub>c</sub> <sup>+</sup>                                | --                         | 0.12               | --                             | [50]      |
| Glycerol -3-phosphate                      | GLY3P  | X <sub>23</sub>            | 0.018              | 0.002                          | [51]      |
| Cytoplasmic glutamate                      | GLU <sub>c</sub>   | X <sub>24</sub>            | 3.766              | 0.013                          | [46]      |
| 4-aminobutyrate                            | GABA   | X <sub>25</sub>            | 0.141              | 0.006                          | [46]      |
| Extracellular glutamate, reduced form      | GLU <sub>e</sub>   | X <sub>26</sub>            | 3.766              | 0.013                          | [46]      |
| Extracellular glutamate, anion form        | GLU <sub>e</sub> <sup>-</sup>                                | --                         | 4.170              | --                             | Estimated |
| Cytoplasmic dihydrogen phosphate           | H <sub>2</sub> PO <sub>4</sub> <sup>-</sup>                  | X <sub>27</sub>            | 2.847              | 0.022                          | Estimated |
| Cytoplasmic hydrogen phosphate             | HPO <sub>4</sub> <sup>2-</sup>                               | --                         | 7.152              | --                             | Estimated |
| Adenosine triphosphate                     | ATP  | X <sub>28</sub>            | 5.28               | 1.164                          | [49]      |
| Adenosine diphosphate                      | ADP  | --                         | 0.47               | --                             | [49]      |
| Adenosine monophosphate                    | AMP  | --                         | 0.09               | --                             | [49]      |
| Intracellular protons                      | H <sup>+</sup>   | X <sub>29</sub>            | 2.51e-5            | 0.086                          | [52]      |
| Nicotinamide adenine dinucleotide reduced  | NADH <sub>m</sub>  | X <sub>30</sub>            | 0.195              | 0.072                          | [50]      |
| Nicotinamide adenine dinucleotide oxidized | NAD <sub>m</sub> <sup>+</sup>                                | --                         | 0.6                | --                             | [50]      |
| Oxygen                                     | O <sub>2</sub>   | --                         | 150 <sub>a</sub>   | --                             | [60]      |
| Flavin adenine dinucleotide reduced form   | FADH <sub>2</sub>  | X <sub>31</sub>            | 0.6 <sup>*</sup>   | 0.002                          | [53]      |
| Flavin adenine dinucleotide oxidize form   | FAD  | --                         | 0.6 <sup>*</sup>   | --                             |           |

Table 1

Table 2.

|                                    | <b>Total</b> | <b>&lt; 1</b> | <b>&lt; 10</b> | <b>&gt;10</b> |
|------------------------------------|--------------|---------------|----------------|---------------|
| <b>L(<math>X_i, X_j</math>)</b>    | 1457         | 1093          | 1441           | 16            |
| <b>L(<math>v_i, X_j</math>)</b>    | 1457         | 1132          | 1455           | 2             |
| <b>S(<math>X_i, r_j</math>)</b>    | 961          | 446           | 891            | 70            |
| <b>S(<math>X_i, r_{jk}</math>)</b> | 10757        | 6960          | 10093          | 664           |
| <b>S(<math>v_i, r_j</math>)</b>    | 961          | 451           | 941            | 20            |
| <b>S(<math>v_i, r_{jk}</math>)</b> | 10757        | 6895          | 10346          | 411           |

Accepted manuscript

$L(X_i, X_j)$ 

| Variables<br>Parameters  | F1,6P<br>(X <sub>4</sub> ) | GAP<br>(X <sub>5</sub> ) | PEP<br>(X <sub>6</sub> ) | PYRc<br>(X <sub>7</sub> ) | OXAc<br>(X <sub>8</sub> ) | MAL <sup>-2</sup> c<br>(X <sub>9</sub> ) | MAL <sup>-2</sup> m<br>(X <sub>10</sub> ) | OXAm<br>(X <sub>11</sub> ) | PYRm<br>(X <sub>13</sub> ) | AcCoA<br>(X <sub>14</sub> ) | C <sub>6</sub> H <sub>5</sub> O <sub>7</sub> <sup>-3</sup><br>(X <sub>15</sub> ) | HC <sub>6</sub> H <sub>4</sub> O <sub>7</sub> <sup>-2</sup><br>(X <sub>18</sub> ) |
|--|----------------------------|--------------------------|--------------------------|---------------------------|---------------------------|--|---|----------------------------|----------------------------|-----------------------------|--|---|
| <i>Cytoplasmic</i><br>HC <sub>6</sub> H <sub>5</sub> O <sub>7</sub> <sup>-2</sup><br><i>transport</i><br>X <sub>61</sub> | -2.617                     | -3.219                   | -2.454                   | -3.138                    | -0.217                    | -2.075                                   | -4.943                                    | -3.835                     | -59.55                     | 1.227                       | 0.709  | 3.367   |
| <i>Mitochondrial</i><br>MAL <sup>-2</sup> -CIT <sup>3</sup><br><i>transport</i><br>X <sub>64</sub>                       | 1.833                      | 2.254                    | 1.723                    | 2.203                     | 0.842                     | 0.520                                    | 3.137                                     | 2.529                      | 29.57                      | -0.664                      | -0.267   | -2.358  |

Table 3

Accepted manuscript

| $L(V_i, X_j)$  |                   |                 |                 |                  |                  |                                 |                                    |                     |                     |                      |   |  |                               |
|--|-------------------|-----------------|-----------------|------------------|------------------|---------------------------------|------------------------------------|---------------------|---------------------|----------------------|---|--|-------------------------------|
| Flux<br>Parameter  | F1,6P<br>$v(X_4)$ | GAP<br>$v(X_5)$ | PEP<br>$v(X_6)$ | PYRc<br>$v(X_7)$ | OXAc<br>$v(X_8)$ | MAL <sup>-2</sup> c<br>$v(X_9)$ | MAL <sup>-2</sup> m<br>$v(X_{10})$ | OXAm<br>$v(X_{11})$ | PYRm<br>$v(X_{13})$ | AcCoA<br>$v(X_{14})$ | C <sub>6</sub> H <sub>5</sub> O <sub>7</sub> <sup>-3</sup><br>$v(X_{15})$ | HC <sub>6</sub> H <sub>5</sub> O <sub>7</sub> <sup>-2</sup><br>$v(X_{18})$ | H <sup>+</sup><br>$v(X_{29})$ |
| <i>Cytoplasmic</i><br>HC <sub>6</sub> H <sub>5</sub> O <sub>7</sub> <sup>-2</sup><br><i>Transport</i><br>X <sub>61</sub> | -2.5              | -2.432          | -2.437          | -2.418           | -2.208           | -2.229                          | -4.972                             | -4.972              | -11.99              | 0.811                | 0.0042  | 1.628  | 0.046                         |
| <i>Mitochondrial</i><br>MAL <sup>-2</sup> -CIT <sup>-3</sup><br><i>Transport</i><br>X <sub>64</sub>                      | 1.751             | 1.703           | 1.711           | 1.698            | 1.313            | 1.302                           | 3.156                              | 3.156               | 5.879               | -0.439               | 0.168   | -0.790   | -0.115                        |

Table 4

Accepted manuscript

**Table 1. Steady state fluxes and metabolite concentration values at steady state in *A. niger* while in citric acid producing conditions.** The main metabolite concentration and fluxes have been taken from [10]. In most instances fluxes have been calculated from known kinetics rates for each enzyme. Values refer at 150 hours of fermentation (idiophase steady state).

(\*)  $\mu\text{mol/mol protein}$

<sup>a</sup>Concentration expressed in millibar.

**Table 2. Sensitivity coefficient and logarithmic gains pattern in *A. niger* citric acid producing conditions steady state.** The distribution of the total number of sensitivities for fluxes ( $v_i$ ) and intermediates ( $X_i$ ), as well as logarithmic gains according with its absolute magnitudes are indicated. For the sensitivities coefficients  $r_j$  refers to the rate constant and  $r_{jk}$  to the kinetics order while in the case of the logarithmic gains  $X_j$  refers to the independent variable, Figures in each column indicate the total number of coefficients (Total) and the number with absolute values below 1; 10 and above 10, respectively.

**Table 3. Concentration Logarithmic Gains.** Influence of cytoplasmic citrate  $\text{HC}_6\text{H}_5\text{O}_7^{2-}$  transport ( $X_{61}$ ) and mitochondrial transport  $\text{MAL}^{2-}\text{-CIT}^{3-}$  ( $X_{64}$ ) on ten representative dependent variables as measured by its Logarithmic Gains.

**Table 4. Flux Logarithmic Gains.** Influence of cytoplasmic citrate  $\text{HC}_6\text{H}_5\text{O}_7^{2-}$  transport ( $X_{61}$ ) and mitochondrial transport  $\text{MAL}^{2-}\text{-CIT}^{3-}$  ( $X_{64}$ ) on ten representative fluxes.

In this work we model the *A. niger* metabolism while in citrate production conditions. It considers information about many cytoplasmic and mitochondria transport processes. The model explains the observed pH homeostasis in *A. niger* while in these conditions. It shed light on the operating molecular mechanisms in *A. niger* and other fungi, bacteria and yeast.

Accepted manuscript